ELSEVIER

Contents lists available at ScienceDirect

Marine and Petroleum Geology

journal homepage: www.elsevier.com/locate/marpetgeo



Geological and geochemical approach to natural hydrogen exploration in the Northern Apennines, Italy

Vivian Azor de Freitas ^{a,b,*}, Alessandra Montanini ^a, Isabelle Moretti ^c, Andrea Artoni ^a, Stefano Segadelli ^d, Jean de la Paix Izerumugaba ^{c,e}, Anne Battani ^c, Giuseppe Etiope ^{f,g}

- a Department of Chemistry, Life Science and Environmental Sustainability, University of Parma, Parco Area delle Scienze,157/a, 43100, Parma, Italy
- b National Agency of Petroleum, Natural Gas and Biofuels (ANP), Avenida Rio Branco 65, 20090-004, Rio de Janeiro, Brazil
- Université de Pau et des Pays de l'Adour, E2S UPPA, LFCR, Pau, France
- ^d Geological, Soil and Seismic Risk Emilia-Romagna Region, Viale della Fiera, 8, 40127, Bologna, Italy
- ^e Université de Pau et des Pays de l'Adour, E2S UPPA, IPREM, Pau, France
- f Istituto Nazionale di Geofisica e Vulcanologia, Sezione Roma 2, Rome, Italy
- g Faculty of Environmental Science and Engineering, Babes-Bolyai University, Cluj-Napoca, Romania

ARTICLE INFO

Keywords: Natural hydrogen exploration Northern Apennines Ophiolites Hyperalkaline water Natural gas

ABSTRACT

The western sector of Northern Apennines, Italy, presents favorable conditions for the occurrence of natural hydrogen (H2), hosting ophiolitic bodies, hyperalkaline waters, and deep-seated faults. A geological and geochemical investigation was conducted to evaluate the potential for subsurface H2 accumulations. The study involved gas analyses from spring waters, bubbling gas, and soil-gas measurements, along with petrographic analyses of ultramafic rocks. Multiple springs contain dissolved H_2 at low (up to 1 μ M) to moderate (1 μ M–100 μM) concentrations relative to other springs in serpentinized peridotites worldwide. In the Taro Valley, H2 occurrences (0.28 µM-0.79 µM) are associated with hyperalkaline springs in proximity to exposed peridotites. However, the limited thickness of the peridotite body at Mt. Prinzera (~250 m) suggests that the hyperalkaline water and associated H₂ likely derive from deeper unexposed ultramafic units. Petrographic analyses of spinelperidotites reveal varying degrees of serpentinization (45 %-95 %), characterized by serpentine mesh textures with olivine relics, pyroxene converted into serpentine, and formation of magnetite and chromite. In the Bobbio Tectonic Window, springs with neutral pH waters, located away from exposed ultramafic bodies, contain higher concentrations of dissolved H2 (0.49 µM-3.8 µM). Although the origin of this H2 remains unclear, it may be related to hidden ultramafic bodies within the sedimentary sequence undergoing serpentinization. Notably, all the spring-related H2 occurrences are associated with methane (CH4), showing thermogenic isotopic signatures $(\delta^{13}\text{C:}58.3 \text{ % to } -35 \text{ % and } \delta^{2}\text{H:}200 \text{ % to } -145 \text{ %})$. Further research should focus on the characterization of regional hydrocarbon reservoirs, which could also host natural H2.

1. Introduction

The goal of the Paris Agreement to keep the global average temperature below 2 $^{\circ}$ C above pre-industrial levels has driven the global transition to low-carbon energy sources, with hydrogen emerging as a prominent alternative. World hydrogen demand could increase by up to 40 % by 2030 in a net zero emissions scenario, driven by the growth of new applications such as power generation, synfuels, and transportation (IEA, 2024). Similarly, hydrogen production, currently dominated by fossil fuels, may be gradually replaced by low-carbon emissions

hydrogen methods, such as electrolysis, steam methane reforming and coal gasification combined with carbon capture. In this context, natural or geological hydrogen (hereafter as natural H₂) represents a potentially cost-effective alternative energy resource compared to manufactured hydrogen, as it is naturally occurring, minimizing the amount of required energy to be produced. Natural H₂ can be generated by a variety of geochemical processes, including serpentinization of ultramafic rocks, different types of oxidations of iron-rich rocks, water radiolysis, thermal degradation of organic matter, mechanoradical reactions along faults, and other minor mechanisms (Zgonnik, 2020; Lévy et al., 2023

E-mail addresses: vivian.defreitasazor@unipr.it, vafreitas@anp.gov.br (V. Azor de Freitas).

https://doi.org/10.1016/j.marpetgeo.2025.107594

Received 5 May 2025; Received in revised form 29 August 2025; Accepted 30 August 2025 Available online 1 September 2025

^{*} Corresponding author. Department of Chemistry, Life Science and Environmental Sustainability, University of Parma, Parco Area delle Scienze, 157/a, 43100, Parma, Italy.

and references therein).

Surface geochemical investigations represent a first step in natural H₂ exploration, as the gas produced and accumulated in underground reservoirs can naturally migrate to the Earth's surface, similar to hydrocarbon seepage, whose studies have allowed the discovery of numerous gas-oil fields throughout the world since the beginning of the 20th century. However, the geological origin of H2 in surface environments (i.e., the identification of H₂ seepage) is not always obvious, as H₂ can also be produced by non-geological mechanisms, such as modern microbial processes (e.g., fermentation) and oxidation of iron-rich sediments in wet soil layers and shallow aquifers (Etiope and Orban, 2025 and references therein). Additionally, corrosion in boreholes (e.g., Feldbusch et al., 2018) and mechanical friction during drilling or hammering for soil-gas sampling can also generate artificial H2 (Davies et al., 2025). Several mechanisms, then, may limit H₂ seepage, especially microbial activity, which often consumes H₂, or the water content in the soil that slows its upward transport (Myagkiy et al., 2020). These factors must be considered in surface H₂ prospection.

Natural H₂ research and exploration are still in an early stage but are rapidly evolving and fostered by the natural H₂ accumulation discovered in Mali, where the gas is extracted at a purity of 98 % (Prinzhofer et al., 2018; Maiga et al., 2023). Since this discovery, multiple studies have been carried out in diverse geological settings around the world (e.g., Guélard et al., 2017; Hao et al., 2020; Boreham et al., 2021; Moretti et al., 2021a and b; Lefeuvre et al., 2022; Leong et al., 2023; Freitas et al., 2024). Industrial projects, including drilling in some cases, are underway in numerous countries, such as Australia, Brazil, Canada, France, Finland, Kosovo, Mali, Oman, South Africa, and the United States (IEA, 2024).

In Italy, studies focusing on natural $\rm H_2$ are still limited. In studies not specifically addressing natural $\rm H_2$, variable concentrations of $\rm H_2$ were detected in a range of environments, including mud volcanoes, springs, volcanic fluids, fluid inclusions, soil, and boreholes (Etiope et al., 2002; Duchi et al., 2005; Tassi et al., 2012; Boschetti et al., 2013; Boulart et al., 2013; Sciarra et al., 2013; Martinelli et al., 2017; Vitale Brovarone et al., 2017; Etiope and Whiticar, 2019; Aiuppa and Moussallam, 2024). Specific investigations on natural $\rm H_2$ were carried out in the Lanzo Peridotite in the Alps, where low $\rm H_2$ concentrations of unknown origin (up to 142 ppmv) were observed in the soil (Dugamin et al., 2019), in the Larderello geothermal field, where 4.5 % of $\rm H_2$ was observed in fumaroles (Leila et al., 2021), and along the Pusteria and Anterselva valleys in the eastern Alps, where up to 1 vol% of $\rm H_2$ in the soil revealed to be non-geological, likely produced by near-surface fermentation (Etiope et al., 2024).

Here, we studied the occurrence of H_2 in springs in the western portion of Northern Apennines in Italy, which exhibits favorable conditions for H_2 occurrences. The widespread presence of ophiolitic bodies hosting ultramafic rocks is highly promising, as these rocks can play an important role in large-scale H_2 from serpentinization. Additionally, the area is characterized by hyperalkaline waters (pH > 9), which could indicate present-day serpentinization occurring underground, deepseated faults, and surface gas manifestations, all favorable aspects for studying H_2 occurrences. However, no dedicated study on natural H_2 exploration has been conducted in this region to date.

To evaluate the H_2 generation potential of this area, we combined geological and hydrogeological data, measurements of H_2 concentrations in springs and surrounding soil, stable C and H isotope composition of CH_4 associated with H_2 , and petrographic studies of the ultramafic rock occurrences.

2. Geological setting and site description

The Northwestern portion of the Apennines forms a NW-SE trending fold-and-thrust belt, extending across Emilia-Romagna, Liguria, and Tuscany. They are part of Mediterranean collisional belts, resulting from the closure of the northern branch of the western Tethys, known as the

Ligure-Piemontese basin. The tectonostratigraphic framework currently observed in the region started with a Mesozoic extensional phase (e.g., Marroni et al., 1998; Stampfli and Borel, 2002; Montanini et al., 2006; Schettino and Turco, 2011; Beltrando et al., 2015; Van Hisenberg et al., 2020; Ferrari et al., 2022) culminating in the Jurassic opening of the Ligure-Piemontese oceanic basin (Tribuzio et al., 2016 and references therein). Following this, the area underwent deformation associated with the convergence of the Adria subplate with the Iberian-Europe plate during the Late Cretaceous to Early Oligocene, forming the Apenninic Belt (Marroni et al., 2017; Conti et al., 2020). The Northern Apennines are primarily composed of sedimentary cover sequences of Mesozoic-Cenozoic age and remnants of the oceanic lithosphere of the Ligure-Piemontese basin, whereas exposures of the pre-Mesozoic basement are rare and mainly limited to scattered occurrences in Tuscany, and in the Punta Bianca, Cerreto and the Alpi Apuane areas (see Pandeli et al., 1994; Molli, 2008; Molli et al., 2020).

The exposed basement of the Northern Apennines consists of low-to medium-grade metamorphic rocks, including phyllites, meta-volcanics, carbonate-siliciclastic metasediments, micaschists, and amphibolites. The metamorphism was attributed to crustal thickening during the collisional phase of the Variscan orogeny locally overprinted during Tertiary Apennine orogenesis (Pandeli et al., 1994; Lo Po,D et al., 2016, 2018; Molli et al., 2002, 2020).

Three main tectonostratigraphic units are recognized in the western part of Northern Apennines, i.e., from bottom to top, Tuscan, Subligurian, and Ligurian units, which are locally overlain by the Epiligurian Succession (Molli et al., 2010; Conti et al., 2020, and references therein; Fig. 1).

The Tuscan units represent the former proximal portion of the Adria western continental margin, known as the Tuscan Domain (Molli, 2008; Molli et al., 2010). They consist of continental successions forming distinct thrust sheets. In particular, the Tuscan Nappe formed as a continental Triassic-Tertiary sedimentary sequence detached from its original basement and unaffected by Alpine metamorphism, while the so-called Tuscan Metamorphic units experienced pre-Alpine (Variscan) and Alpine metamorphism mostly under greenschist facies conditions (Franceschelli et al., 2004; Molli et al., 2020). The topmost portion of the Tuscan Unit is made of siliciclastic turbidites, sandstone, and carbonates deposited from the Late Oligocene to Early Miocene (Conti et al., 2020 and references therein); foredeep sequences related to the Apenninic Orogeny. Based on the age of the Early Miocene foredeep deposits, overlaying the Tuscan Metamorphic Succession, the Tuscan Unit can be subdivided into two subunits (Fig. 1): the Tuscan Succession, the deposits being youngest foredeep Aquitanian, Cervarola-Falterona Succession, the youngest foredeep deposits being Burdigalian.

During the Early Paleocene to Early Miocene, deep marine deposits constituted the Subligurian unit, which, from Late Eocene, were progressively superimposed by the Ligurian unit, and both overthrust the Tuscan and Cervarola-Falterona units (Ogata et al., 2012; Conti et al., 2020; Piazza et al., 2020).

The Ligurian units consist of ophiolitic sequences, which represented the oceanic lithosphere of the Ligure-Piemontese basin and sedimentary deposits formed between Late Cretaceous and Eocene in an accretionary prism (Marroni and Pandolfi, 1996; Marroni et al., 2017). They are subdivided into Internal and External Ligurian, related to distal and proximal domains of the Ligure-Piemontese oceanic basin, respectively (Sanfilippo and Tribuzio, 2011). The Internal Ligurian ophiolites are not associated with continental material and consist of gabbro-peridotite basement overlain by volcano-sedimentary sequences (Sanfilippo and Tribuzio, 2011). The Bracco-Levanto is one of the major ophiolitic bodies of Internal Ligurian units, where serpentinized peridotites, gabbros, and ophicalcites are exposed (Tribuzio et al., 1997). The External Ligurian ophiolites occur as slide-blocks in sedimentary mélanges (Marroni et al., 1998) that formed during the inception of convergence-related sedimentation in Late Cretaceous times (Marroni

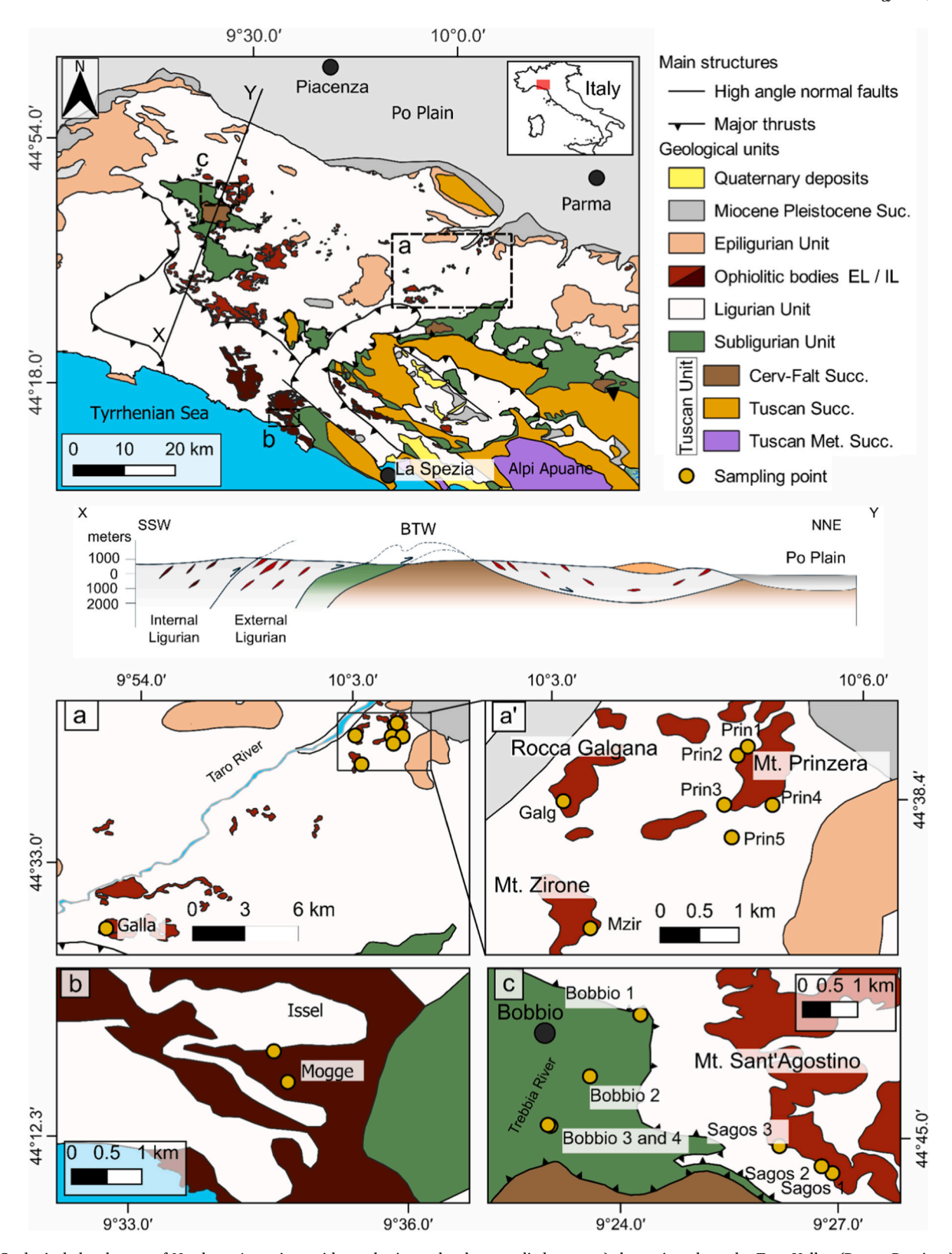


Fig. 1. Geological sketch map of Northern Apennines with emphasis on the three studied areas: a) the region along the Taro Valley (Parma Province), a') Mt. Prinzera region in detail, b) Castagnola (La Spezia Province), and c) Bobbio (Piacenza Province). The yellow circles correspond to the 17 visited sites, the red polygons refer to the ophiolitic bodies within the External Ligurian (EL), and the dark red ones correspond to the ophiolite bodies of the Internal Ligurian (IL). Geological units were based on Conti et al. (2020), main structures modified from Molli (2008), and ophiolite bodies were based on the Geological Map of Northern Apennines (Servizio Geologico d'Italia, 2005; Servizio Geologico d'Italia, 1997; Conti et al., 2020). Tuscan Nappe, Cervarola-Falterona, and Tuscan Metamorphic Successions are comprised of the Tuscan units (Conti et al., 2020). Schematic regional cross-section extending from the Internal Ligurian Unit to the Po Plain, crossing the Bobbio Tectonic Window, adapted after Marroni et al. (2010, 2019). (For interpretation of the references to colour in this figure legend, the reader is referred to the Web version of this article.)

et al., 2017). In these ophiolites, exhumed subcontinental mantle (Montanini et al., 2006; Rampone et al., 1995) is associated with MOR-type gabbroic and basaltic rocks (Montanini et al., 2008) and, locally with continental crust material. The mantle bodies are up to a few km lateral extent and are composed of spinel-plagioclase lherzolites with pyroxenite layers (Montanini et al., 2006; Ferrari et al., 2022). The ophiolitic bodies are mainly exposed in the Piacenza area and along the Taro Valley in the Parma Province (Fig. 1; see Montanini et al., 2006; Salvioli-Mariani et al., 2020; Ferrari et al., 2022).

The Epiligurian Succession originated from a piggy-back basin with sedimentary units deposited unconformably on the Ligurian units between the Middle Eocene and Late Miocene/Early Pliocene (Piazza et al., 2016; Conti et al., 2020).

2.1. Description of the studied sites and field relations

In the western Northern Apennines, three areas were chosen as study sites: the region along the Taro Valley (Parma Province), Castagnola (La Spezia Province), and Bobbio (Piacenza Province) (Fig. 1).

Along the Taro Valley, two hyperalkaline springs associated with ophiolitic bodies were investigated (Fig. 1a): Galla (pH 10.3) in Groppo di Gorro locality and Prin2 in Mt. Prinzera, showing pH of 11.2 and dissolved $\rm H_2$ previously reported by Boschetti et al. (2013). Additional springs with neutral to slightly alkaline pH (7.5–8.8) have also been investigated (Prin1, Prin3, Prin4, Prin5, Galg), including a groundwater sample from about 13 m deep in a borehole in the Mt. Zirone (Mzir).

Prin2 and Galla springs correspond, respectively, to sodium-sulfate and sodium-hydroxide waters, with high pH (10.3–11.2), low Eh (up to $-103~\rm mV$) and high B/Cl ratios (higher than 13000 mg/L) (Boschetti and Toscani, 2008). The other springs studied in the Mt. Prinzera region exhibit a Mg-HCO $_3$ composition, with intermediate pH values ranging from 7.5 to 8.8, fresh salinity (228 mg/L), and positive redox potential (from 90 to 565 mV) (Segadelli et al., 2017a).

In the Castagnola area, we investigated a hyperalkaline spring water (Issel) and a managed spring with pH 8.6 (Mogge), both situated in the Bracco-Levanto ophiolitic massif (Fig. 1b). Issel corresponds to a sulfide-bearing spring (Fantoni et al., 2002) with high pH (>10) and negative Eh (-220.4 mV).

In the Bobbio region, two areas were tested: springs in the ultramafic body of Mt. Sant' Agostino and additional springs in the sedimentary successions of Bobbio Tectonic Window (BTW) along the Trebbia River (Fig. 1c). The last area was selected due to the presence of deep faults and gaseous manifestations previously reported (Scicli, 1972; Martinelli et al., 2012), including bubbling springs in the old thermal baths of Bobbio (Bobbio3 and Bobbio4). These baths, closed over 20 years ago, still preserve the ruins of the original building.

Along the Trebbia River (Bobbio1 to 4), the springs are thermal (20 $^{\circ}$ C-30 $^{\circ}$ C) and contain chlorine-sodic waters as a result of mixing with Cl-rich fossil marine waters, possibly originated by the dissolution of Triassic evaporites, which remained trapped in sedimentary layers during the Apennine orogeny (Duchi et al., 2005; Boschetti et al., 2011). In Mt. Sant' Agostino, the springs (Sagos1, Sagos2, and Sagos3) have slightly alkaline waters (pH 8.2 to 8.5) and a Mg-HCO $_3$ composition (data provided by the water management company IRETI S.p.a.).

2.1.1. Ultramafic bodies

The km-sized mantle bodies of Mt. Prinzera-Mt. Zirone and Mt. Sant'Agostino (Fig. 1c) are composed of variably serpentinized spinel-plagioclase foliated peridotites. Their textures vary from porphyroclastic to mylonitic and ultramylonitic. The most preserved outcrops are characterized by relatively large (up to 1 cm across) pyroxene porphyroclasts. Pyroxenite layers concordant with the foliation of the host peridotite, mainly ranging in thickness from a few millimeters to 8–10 cm, are widespread. At Mt. Prinzera, brittle deformation with multiple stages of veining, hydration, and local formation of tectonic breccias is common (see Montanini et al., 2006; Segadelli et al., 2017b for a

detailed description).

The Groppo di Gorro body forms a km-sized outcrop with a thickness of 150–200 m (see Salvioli-Mariani et al., 2020 and quoted references). Here, the original mantle rocks have undergone extensive serpentinization and are now composed of massive to intensely fractured serpentinites. Pyroxene porphyroclasts and Cr-spinels with whitish rims of altered plagioclase have been locally preserved. Cataclastic texture and complex serpentine-carbonate veining patterns may occur along the margins of the body.

The Bracco-Levanto ophiolite consists of a gabbroic pluton intruded into mantle peridotites (Sanfilippo et al., 2014). In the Issel spring area (Fig. 1b), the exposed mantle rocks are dark gray, massive serpentinites with rare relics of orthopyroxene porphyroclasts.

2.1.2. Bobbio Tectonic Window

In the westernmost part of the Northern Apennines, the Bobbio Tectonic Window exposes the Cervarola-Falterona Succession, and it is surrounded by the Ligurian and Subligurian units (Servizio Geologico d'Italia, 1997; Ogata et al., 2012).

The Cervarola-Falterona units are represented by siliciclastic turbidites of the Bobbio Formation, slumped deposits of Marsaglia Complex, both Miocene in age, overthrust by the Late Eocene-Early Miocene hemipelagites and turbidites of the Salsominore Formation and finegrained turbidites of the Rio Fuino Sandstone (Labaume, 2011).

The Subligurian units bordering the BTW correspond to Val D'Aveto Formation, an Oligocene turbiditic complex that also includes conglomerates with volcanic clasts (basalt, andesite, and rhyolite, Mattioli et al., 2002) and calcareous and siliciclastic turbidites of Paleocene-Eocene Canetolo Unit.

The Ligurian units comprise deep marine mass and gravitational flow deposits of the Monte Ragola and Monte Veri Cretaceous complex (i.e., External Ligurian ophiolites), which are associated with ultramafic olistoliths (Servizio Geologico d'Italia, 1997; Labaume, 2011). The ultramafic bodies of Monte Sant' Agostino and Monte Gavi, north-eastwards, and Monte Ragola, south-eastwards, are some mantle bodies exposed around the BTW (Ferrari et al., 2022).

3. Material and methods

 $\rm H_2$ occurrence was investigated in 16 springs and one borehole (Fig. 2), located in the three areas indicated in Fig. 1. The presence of $\rm H_2$ was also checked in the soil around some springs, and mineralogical analysis of exposing ultramafic rocks was carried out, as described below.

3.1. Sampling and laboratory analysis of dissolved gas in spring water

Water samples from 16 springs (Fig. 2a-d) and one borehole (Fig. 2e) were collected in 2019, 2023, and 2024 in 500 mL Duran borosilicate glass bottles capped with bromobutyl rubber stopper. In the laboratory, the dissolved gas was extracted using the equilibrium headspace method (Capasso and Inguaggiato, 1998), and the concentrations of H2, CH4, and CO2 were measured. H2 was quantified using a semiconductor + pellistor sensor (Huberg Metrex 2, Italy; lower detection limit 5 ppmv; range 0-5 vol%; accuracy \leq 2 % at 1000 ppmv, and \leq 1 % at 10,000 ppmv; measurements checked with 100 and 1000 ppmv H₂ standards), while CH₄ and CO₂ were analyzed using a Tunable Diode Laser Adsorption Spectrometry (TDLAS) detector (Gazomat, France; uncertainty 0.1 ppmv, lower detection limit 0.1 ppmv; range 0-100 vol%) and a Licor non-dispersive infrared sensor (Licor LI-820; accuracy <3 % of reading; range 0–20,000 ppmv). To prevent seal damage and possible H_2 leakage from the bottles, the interval from sampling to gas analysis regardless of the collection date — ranged from one to eight weeks. During this period, the bottles were stored in a refrigerator at 4 °C until analysis.

Stable carbon and hydrogen isotope compositions of CH₄ (δ^{13} C vs.



Fig. 2. Photographs illustrating various sampling methods and spring water types: a) natural spring water, exhibiting a white track in the wall (Bobbio1); b) hyperalkaline spring water coming out of ophiolitic rocks (Issel), c) tapped spring water sampling (Sagos3); d) bubbling spring water forming a pond close to the Trebbia River's margin (Bobbio4); e) borehole water sampling (Mzir), and f) bubbling spring gas sampling (Bobbio3).

VPDB and $\delta^2\mathrm{H}$ vs. VSMOW), extracted from Bobbio1 and Bobbio2, were analyzed using, respectively, an Agilent 6890N GC coupled to a Finnigan Delta S Isotope Ratio Mass Spectrometer (IRMS) via a GC-Isolink or a Finnigan GC-C III interface from Thermo (uncertainty of <0.2 ‰), and an Agilent 7890A GC coupled to a MAT 253 IRMS via a GC-isolink interface from Thermo (uncertainty of <1 ‰).

The isotopic composition of CH₄, extracted from Bobbio3 and Bobbio4 water samples, was analyzed on an automated IRMS system (Brass and Röckmann, 2010; Röckmann et al., 2016) with a typical uncertainty of <0.1 ‰ for $\delta^{13} C_{\text{CH4}}$ and <2 ‰ for $\delta^{2} H_{\text{CH4}}$. The system has been validated in international intercomparison programs (Umezawa et al., 2018). The stable carbon isotopic compositions of CH₄ and CO₂ ($\delta^{13} \text{C}$ vs. VPDB), extracted from water samples of Prin1, Prin2b, and Galla, were analyzed by Cavity Ring-Down Spectroscopy (CRDS) using a Picarro G2201-I C isotope analyzer (Picarro Inc., USA; uncertainty <0.4 % for $\delta^{13} \text{C-}_{\text{CH4}}$ and <0.12 % for $\delta^{13} \text{C-}_{\text{CO2}}$). The measurements were also checked and confirmed using two certified isotope standards ($\delta^{13} \text{C-}_{\text{CH4}}$: 39.4 ‰ and +19.4 ‰ VPDB) from the Biogeochemical Laboratories of Indiana University.

3.2. Sampling and laboratory analysis of free gas

Three gas samples were collected as bubbles from the springs

Bobbio1, Bobbio3 (Fig. 2f), using a multi-layer foil bag, and Bobbio4, using the classic inverted funnel system and sampling into a copper tube, which was tightly clamped at both ends to ensure no leakage or contamination.

For Bobbio1 and Bobbio3, the stable carbon isotopic composition of CH₄ and CO₂ (δ^{13} C vs. VPDB) was analyzed by CRDS using the same methodology for dissolved gas samples Prin1, Prin2b, and Galla described in section 3.1.

The Bobbio4 bubble gas sample was analyzed with an Agilent 6890N/7890A/7890B gas chromatograph (GC). The $\rm H_2, O_2+Ar, N_2,$ and CH $_4$ were measured on the cited GC equipped with a 12 m, 0.32 mm molsieve column (Agilent), a heated injection valve and a TCD detector. Hydrocarbons and CO $_2$ were analyzed on the GC equipped with a 50 m, 0.32 mm Porabond-Q column (Agilent), a heated injection valve, a heated backflush valve (for C $_{6+}$), a TCD detector (for CO $_{2}$) and an FID detector (for hydrocarbons). Stable carbon and hydrogen isotopes of methane and carbon dioxide were analyzed using the same methodology applied for dissolved gas samples.

3.3. Measurements of pH

The water pH was measured in the field using a portable instrument HQ Series multi-meter equipped with a PHC101 sensor (measure range:

2–14 pH, accuracy of ± 0.02 pH) for Issel and Mogge springs, and using a Hanna HI991300 pH meter (measure range: 2 to 16 pH, accuracy of ± 0.1 pH) for Galg, Bobbio1, 2, 3 and 4 springs. In the case of Prin3, 4 and 5, the pH was measured in the laboratory four weeks after sampling using an XS PC70 (measurement range: 2 to 16 pH, accuracy of ± 0.02 pH). For Prin1, Prin2a, b, and c and Galla pH data are from Boschetti et al. (2013), in which the springs are referred to as PR01, PR10, and UM15, respectively. For the borehole water from Mt. Zirone (Mzir), the mean pH values reported in Regione Emilia-Romagna, Regione (2016) were considered. The pH data for the springs Sagos1, 2, and 3 were provided by the company IRETI S.p.a., which manages the springs as drinking water sources.

3.4. On-site measurements of H_2 in soils

Twelve measurements of H_2 in soil gas were carried out around the six selected springs, Prin2, Prin3, Galg, Bobbio4, Sagos1, and Sagos2, to check possible H_2 concentrations in the soil. The measurements were performed in July 2023 using the portable instrument BIOGAS5000 from Geotech®. The distance between the soil-gas measurements and the springs is approximately a few meters for all sites except for Prin3, which is about 80 m away. The sensor measurement's range is 0–1000 ppmv (± 10.0 %FS) for H_2 . At each site, a hole 80 cm deep and 1 cm wide was drilled in the soil using a portable drilling machine from Bosch® in percussion mode.

3.5. Rock investigations

Ultramafic rock samples from the studied ophiolitic bodies, i.e., Mt. Prinzera, Mt. Zirone, Rocca Galgana, Mt. Sant' Agostino, Groppo di Gorro, and Bracco-Levanto, were selected for petrographic analyses. Their thin sections were examined under transmitted light using a Leitz optical microscope. Given that serpentinization of ultramafic rocks is a well-known process for natural H_2 generation in the subsurface, the petrographic study focused on identifying the primary minerals involved in this process and their textural relationships. For this purpose, the serpentinization degree and concentrations of olivine and pyroxene were estimated, and we searched for accessory minerals such as brucite and magnetite.

4. Results

4.1. Dissolved gas in the investigated groundwaters

In the Taro Valley, three springs (Prin2, Prin3, and Galla; Fig. 1a) exhibit variable amounts of dissolved H2 (from 0.28 µM to 0.79 µM; Table 1), while H₂ was below the detection limit in the remaining spring waters from Mt. Prinzera and the nearby ophiolitic bodies (Rocca Galgana and Mt. Zirone). In Mt. Prinzera, the hyperalkaline spring water Prin2, which contains significant amounts of CH_4 (42.44–83.75 μM) and CO2 below the Air Saturated Water (ASW) level, was sampled at three different times: during the fall-winter of 2010/2011 (Prin2c, Boschetti et al., 2013), in summer-autumn of 2019 (Prin2b) and during the summer of 2023 (Prin2a). H₂ was found dissolved in the water during all sampling campaigns, regardless of the season and the difference of more than 12-year gap between sampling events. The Prin2b sample displays the highest amounts of dissolved H_2 (0.79 μM). Dissolved H_2 was also detected in Prin3 (0.44 µM), a neutral spring (pH 7.7), which, like Prin2, is located on the western side of Mt. Prinzera. In the Groppo di Gorro ophiolitic body, located 22 km southwest of Mt. Prinzera, the Galla hyperalkaline spring contains 0.67 µM of dissolved H₂, similar to the Prin2b sample. However, it exhibits lower amounts of CH₄ (5.63 μM). The stable carbon isotopic composition of CH₄, $\delta^{13}C_{CH4}$, measured in Prin1, Prin2, and Galla samples, ranges from -58.3 % to -39 %.

In the Castagnola area (Bracco-Levanto ophiolitic body; Fig. 1b), $\rm H_2$ concentration is below the detection limit both in the hyperalkaline spring water of Issel and in the Mogge spring, characterized by a pH of 8.6. The CH₄ concentration is higher (1.13 μ M) in the hyperalkaline spring (with CO₂ below the ASW level) compared to the Mogge spring (0.09 μ M of CH₄ with 26.8 μ M of CO₂).

In the Bobbio region (Fig. 1c), along the Trebbia River, dissolved $\rm H_2$ was detected in three different springs (Bobbio1, 3, and 4), ranging from 0.49 μM to 3.86 μM . Here, $\rm H_2$ is associated with variable amounts of CH₄ (47.6 μM –361.3 μM) and CO₂ (237.6 μM –496.2 μM). In Bobbio1 and Bobbio2 springs, the $\delta^{13}C_{\rm CH4}$ values range from –35.1 % to –35 %, and the $\delta^2 H_{\rm CH4}$ values are from –157 % to –145 %. Bobbio3 and 4 exhibit higher $\delta^{13}C$ and $\delta^2 H$ values ranging from –26.7 % to –25.8 % and –50.2 % and –46.5 %, respectively. In three springs at the base of the ophiolitic massif of Mt. Sant' Agostino (Sagos1, 2 and 3), dissolved $\rm H_2$ is

Table 1 Concentrations of CH₄, H₂, and CO₂ (μM) dissolved in the groundwater and stable carbon (δ^{13} C ‰, VPDB) and hydrogen (δ^{2} H ‰, VSMOW) isotope composition of CH₄ for the three investigated areas. All sites correspond to water springs, except for the water sample Mzir collected from a borehole at a depth of 13 m.

Sample	Site	Latitude	Longitude	pH	CH ₄	H_2	CO_2	$\delta^{13}C_{CH4}$	$\delta^2 H_{CH4}$
a) Taro Valle	ey								
Prin1	Mt. Prinzera	44°38′54.54″	10°4′53.33″	8.8	1.13	b.d.l.	nm	-44.0	nm
Prin2a	Mt. Prinzera	44°38′48.92″	10°4'46.55"	11.2	42.44	0.33	<asw< td=""><td>nm</td><td>nm</td></asw<>	nm	nm
Prin2b	Mt. Prinzera	44°38′48.92″	10°4'46.55"	11.2	83.75	0.79	nm	-55.0	nm
Prin2c ^a	Mt. Prinzera	44°38′48.92″	10°4'46.55"	11.2	73.13	0.28	<asw< td=""><td>-58.3</td><td>-200</td></asw<>	-58.3	-200
Prin3	Mt. Prinzera	44°38′54.54″	10°4′53.33″	7.7	0.57	0.44	<asw< td=""><td>nm</td><td>nm</td></asw<>	nm	nm
Prin4	Mt. Prinzera	44°38′20.92″	10°5′7.57″	7.7	0.00	b.d.l.	70.2	nm	nm
Prin5	South of the Mt. Prinzera	44°38′2.23″	10°4'44.09"	7.5	0.01	b.d.l.	126.1	nm	nm
Galg	Rocca Galgana	44°38′23.08″	10°3′06.75″	8.0	0.02	b.d.l.	52.2	nm	nm
Galla	Groppo di Gorro	44°30′10.44″	9°52′29.79″	10.3	5.63	0.67	nm	-39	nm
Mzir	Mt. Zirone	44°37′10.21″	10°3′22.70″	8.0	0.05	b.d.l.	19.1	nm	nm
b) Castagnol	a area								
Issel	Bracco-Levanto	44°13′12.27"	9°34′33.72″	11.1	1.13	b.d.l.	<asw< td=""><td>nm</td><td>nm</td></asw<>	nm	nm
Mogge	Bracco-Levanto	44°12′52.55″	9°34′42.67″	8.61	0.09	b.d.l.	26.8	nm	nm
c) Bobbio ar	ea								
Bobbio1	Piancasale	44°46′42.48″	9°24′16.37″	8.0	47.63	0.49	287.3	-35.0	-157.0
Bobbio2	Rio Foino	44°45′51.43″	9°23′34.46″	7.2	361.25	b.d.l.	237.6	-35.1	-145.0
Bobbio3	Old thermal baths	44°45′9.78″	9°23′1.77″	7.2	89.56	3.86	428.2	-25.8	-46.5
Bobbio4	Old thermal baths	44°45′11.53″	9°22′59.05″	7.6	174.00	0.90	496.2	-26.7	-50.2
Sagos1	Sant'Agostino	44°44'31.29"	9°26′55.10″	8.2	0.00	b.d.l.	62.6	nm	nm
Sagos2	Scabiazza	44°44′36.89″	9°26′46.71″	8.5	0.07	b.d.l.	<asw< td=""><td>nm</td><td>nm</td></asw<>	nm	nm
Sagos3	Monte1 and 2	44°44′52.72″	9°26′8.62″	8.2	0.07	b.d.l.	36.4	nm	nm
Air Saturated Water (ASW) at 20 °C					0.0025	0.0004	14.5		

a Data from Boschetti et al. (2013)b.d.l.: below the detection limit (corresponding to 5 ppmv H2 in the extracted gas phase), nm: not measured.

below the detection limit, CH_4 concentrations were up to 0.07 $\mu\text{M},$ and CO_2 levels up to 62.6 $\mu\text{M}.$

4.2. Free gas in bubbling springs

The free gas samples (Bobbio1, Bobbio3, and Bobbio4) correspond to numerous discontinuous bubble gas flows, each lasting a few seconds. The bubbling gas from Bobbio4 was sampled during the summer of 2023, while Bobbio1 and Bobbio3 sampling was conducted during the autumn of 2024.

The bubbling gas in Bobbio4 is mainly composed of CH₄ (97.4 %) and CO_2 (1.8 %; Table 2). The H₂ level was below the GC detection limit (400 ppmv).

The stable carbon isotopic compositions (δ^{13} C) of CH₄ and CO₂ measured in these free gas samples range from -35.8 % to -35.7 % and from -27 % to -21.4 %, respectively, while δ^2 H_{CH4} in Bobbio4 was -152 % (Table 3).

4.3. Gas concentration in the soil

Soil-gas measurements detected some levels of $\rm H_2$ across all analyzed sites (Table 4), but the values remain low. $\rm H_2$ concentrations ranged from 4 ppmv to 17 ppmv, with the lowest values observed in the Mt. Prinzera springs (Prin2 and Prin3), where dissolved $\rm H_2$ was detected. The highest soil-gas concentrations were found in the Rocca Galgana spring (Galg), where dissolved $\rm H_2$ was below the detection limit.

4.4. Petrographic characterization of ultramafic rocks

The peridotites from Mt. Prinzera and nearby bodies (Rocca Galgana, Mt. Zirone) display similar petrographic features. They have foliated textures, ranging from porphyroclastic to mylonitic. They have undergone variable degrees of serpentinization (45 %–95 %). Porphyroclastic texture prevails, showing porphyroclasts of olivine, clinopyroxene, and orthopyroxene (up to 10 mm) embedded in a fine-grained matrix (Fig. 3a). This matrix is mainly formed by serpentine and olivine in a mesh texture and by recrystallized pyroxenes and minor spinel. Only pseudomorphs after olivine and pyroxene are discernible in the most serpentinized samples. Cr-spinel may also occur as porphyroclasts, sometimes with plagioclase rims (Fig. 3a). Disseminated brown amphibole may occur as an accessory phase. Magnetite (Fig. 3b) occurs in some samples associated with serpentine. Brucite was not identified in the analyzed thin sections.

In the Groppo di Gorro ultramafic body, the degree of serpentinization is generally high (mostly from 80 % to 100 %), but relatively fresh samples (serpentinization ca. 50 %) have been locally found. They display an isotropic, coarse-grained granular texture with large porphyroclasts of exsolved ortho- and clinopyroxenes and olivine (as relics in a mesh-texture, Fig. 3c). Dark brown Cr-spinel is mantled by altered plagioclase, which also occurs as disseminated patches. More frequently, olivine was entirely replaced by serpentine with a mesh texture, which was subsequently replaced by chlorite. Orthopyroxenes were typically converted into fibrous gray serpentine (bastite), while spinel is transformed into opaque Mg-chromite (±chlorite) with altered plagioclase rims.

The peridotites outcropping in the Castagnola locality, belonging to the Levanto-Bonassola ophiolite (Sanfilippo et al., 2014), are massive rocks, extensively serpentinized. Olivine was replaced by mesh-texture

Table 3Isotopic data of the bubbling springs in the Bobbio region.

Sample	$\delta^{13} C_{CH4}$	$\delta^{13} C_{CO2}$	$\delta^2 H_{CH4}$
Bobbio1	-35.8	-27	nm
Bobbio3	-35.7	nm	nm
Bobbio4	-37.5	-21.4	-152

Isotopic data: $\delta^{13}C_{CH4}$ and $\delta^{13}C_{CO2}$ in permil (‰), VPDB; δ^2H_{CH4} permil (‰), VSMOW. nm: not measured.

Table 4Soil-gas H₂ concentrations around six springs.

Sample	Site	H ₂ ppmv
Prin2	Monte Prinzera	4
		5
Prin3	Boschi di Bardone	4
Galg	Rocca Galgana	9
		15
		17
Bobbio4	Bubbling spring old thermal baths	8
		10
Sagos1	Sant'Agostino Sanctuary	5
		7
Sagos2	Spring water Scabiazza	9
		11

serpentine, pyroxenes were replaced by fibrous, bastite-like serpentine with rare relics, and spinel was transformed into opaque Mg-chromite.

5. Discussion

5.1. Evaluation of H_2 concentration data

Hyperalkaline springs associated with serpentinized ophiolitic rocks frequently (but not always) contain measurable amounts of $\rm H_2$ (e.g., Boulart et al., 2013; Etiope et al., 2013; Pasquet et al., 2025). However, this amount is not constant and may vary over time. For instance, at the same spring in the Semail ophiolites, the $\rm H_2$ content varied from below the detection limit (i.e., 400 ppmv) to 44.6 % (after air correction) over five months (Pasquet et al., 2025). The paucity of $\rm H_2$ in some CH₄-bearing hyperalkaline waters may result from complete microbial or abiotic $\rm H_2$ consumption through $\rm CO_2$ reduction in a limited $\rm H_2$ production system.

Dissolved H_2 was observed in the hyperalkaline springs of Prin2 and Galla, whereas it was below the detection limits in Issel. Among ophiolite-related sites with lower pH values (7.5–8.8), the only site where dissolved H_2 was detected corresponds to the Prin3 spring, which is located at the base of Mt. Prinzera, about 900 m southwest of Prin2.

In Prin2b, Prin3, and Galla, H_2 concentrations are of the same order of magnitude or slightly higher than the level of H_2 that, according to literature (Etiope and Orban, 2025), can be attributed to near-surface microbial origin (up to 0.426 μ M). Two of the three H_2 measurements in Prin2 (Prin2a and Prin2c) showed levels below the microbial range, suggesting either variability in the geological H_2 input or partial or complete microbial H_2 consumption.

Most of the springs in the Bobbio area contain higher amounts of dissolved $\rm H_2$ than the ophiolite-related hyperalkaline springs studied here. The exception is the Bobbio2 spring, which exhibits dissolved $\rm H_2$ concentration below the detection limit and a higher concentration of

Table 2Gas concentrations of the bubbling spring Bobbio4.

Sample	CH ₄	C ₂ H ₆	N ₂	CO_2	H ₂	H ₂ S	CO	O ₂ +Ar	Air correction %
Bobbio4	97.4	0.017	0	1.8	nd	nd	nd	0.72	40.3

Gas composition is in vol% corrected for air. The air correction was based on the original N_2 , O_2 and Ar concentrations. nd: not detected. Ethene and C_{3+} hydrocarbons are present in total concentrations of less than 0.004 vol%.

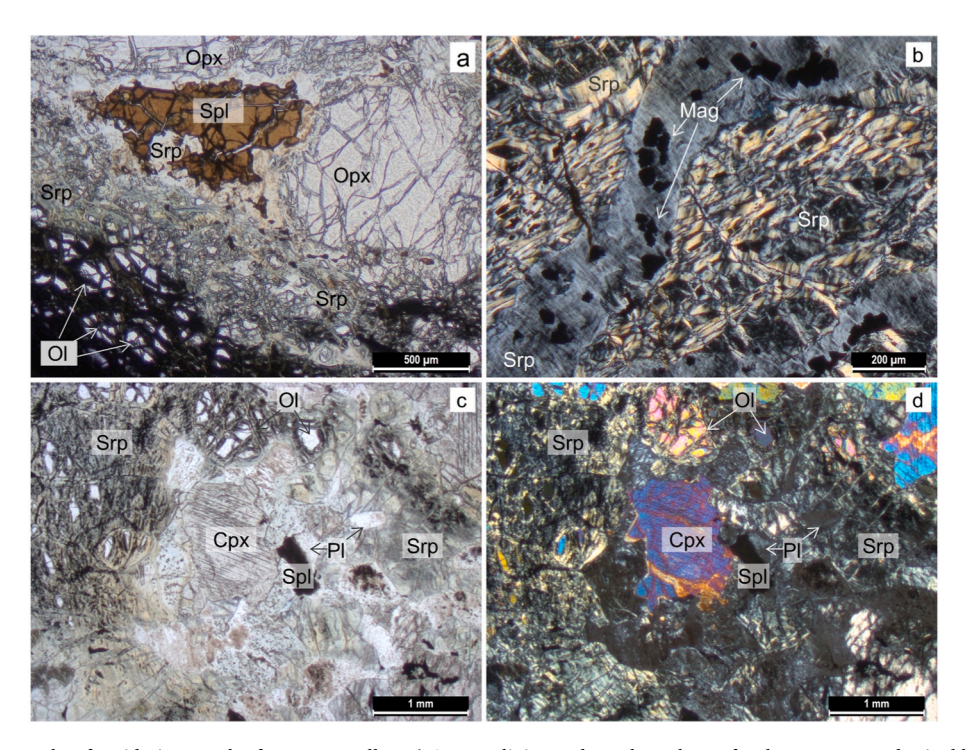


Fig. 3. Thin section photographs of peridotite samples from Taro Valley. a) Coarse olivine and porphyroclasts of orthopyroxene and spinel bordered by serpentine in peridotite sample from Mt. Prinzera (parallel nicols). b) Serpentine in a mesh texture with hourglass core cut by serpentine vein containing magnetite in peridotite sample from Mt. Prinzera (crossed nicols). c) and d) parallel and crossed nicols, respectively, coarse-grained peridotite of Groppo di Gorro, exhibiting porphyroclasts of exsolved ortho- and clinopyroxenes, olivine as relics in a mesh-texture; dark brown Cr-spinel bordered by altered plagioclase, which also occurs as disseminated patches. Mag: magnetite; Ol: olivine; Cpx: clinopyroxene; Opx: orthopyroxene; Pl: plagioclase; Srp: serpentine; Spl: spinel. (For interpretation of the references to colour in this figure legend, the reader is referred to the Web version of this article.)

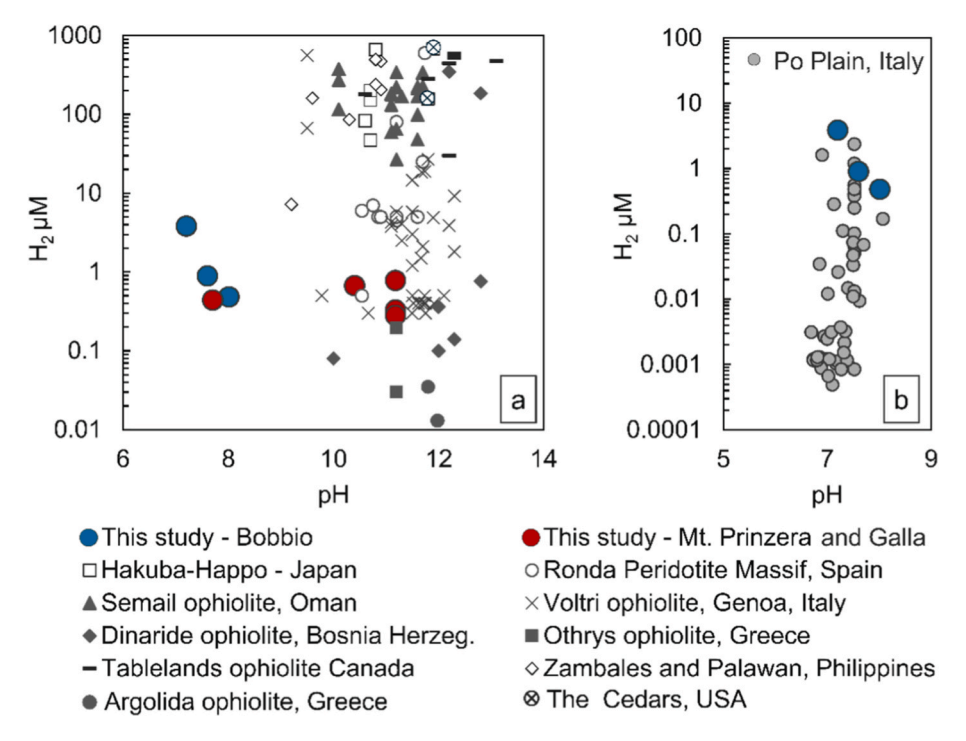


Fig. 4. Binary diagram exhibiting dissolved H₂ concentrations versus pH from different springs and wells. a) Dissolved H₂ concentrations in hyperalkaline springs worldwide compared with the results obtained in this study. World data from Schwarzenbach (2011), Boulart et al. (2013), Etiope et al. (2013), Szponar et al. (2013), Suda et al. (2014), Cardace et al. (2015), Etiope et al. (2016), Brazelton et al. (2017), Etiope et al. (2017), D'Alessandro et al. (2018), Cook et al. (2021); Ojeda et al. (2023). b) Dissolved H₂ levels versus pH for the Bobbio samples compared to Po plain well data (Italy), located in Northern Italy and showing similar pH values (Sciarra et al., 2013; Martinelli et al., 2017).

dissolved CH_4 compared to the other springs in the same region. The occurrence of dissolved H_2 along Trebbia River in Bobbio was unexpected, as it lies within a structural window, with ophiolitic bodies exposed several km away at a higher structural position. The springs exhibit neutral pH values (7.2–8.0), initially not suggesting ongoing serpentinization in the subsurface.

The concentrations of dissolved H_2 observed in this study are relatively low (up to 1 μ M), whereas one sample (Bobbio3) exhibits intermediate levels (1 μ M–100 μ M) compared to hyperalkaline springs associated with ultramafic rocks worldwide (Fig. 4a). Consistently higher concentrations were found in Semail (Oman), The Cedars (USA), Tablelands (Canada), Zambales and Palawan (Philippines) ophiolites, and Hakuba-Happo (Japan) hot springs related to serpentinites. In the ophiolites of Voltri (Italy), Ronda (Spain), and Dinaride (Bosnia and

Herzegovina), a few springs exhibit very high concentrations of dissolved $H_2\,(>\!100\,\mu\text{M})$, although most sites displayed low to intermediate levels. Dissolved H_2 concentrations in Greece's Othrys and Argolide ophiolites are lower than those measured in this study.

The dissolved $\rm H_2$ concentrations from Bobbio were also compared with dissolved gas from Po Plain wells (Fig. 4b; Sciarra et al., 2013; Martinelli et al., 2017), located in northern Italy, approximately 125 km–160 km to the east of Bobbio. Notably, the dissolved $\rm H_2$ concentrations in the Bobbio region are higher than most wells observed in Po Plain, which also exhibits neutral pH values and is not linked directly to ophiolitic formations.

Nonetheless, while comparisons between worldwide values are informative, it is important to consider that other factors can influence H_2 solubility, such as temperature, pressure, and salinity. In particular,

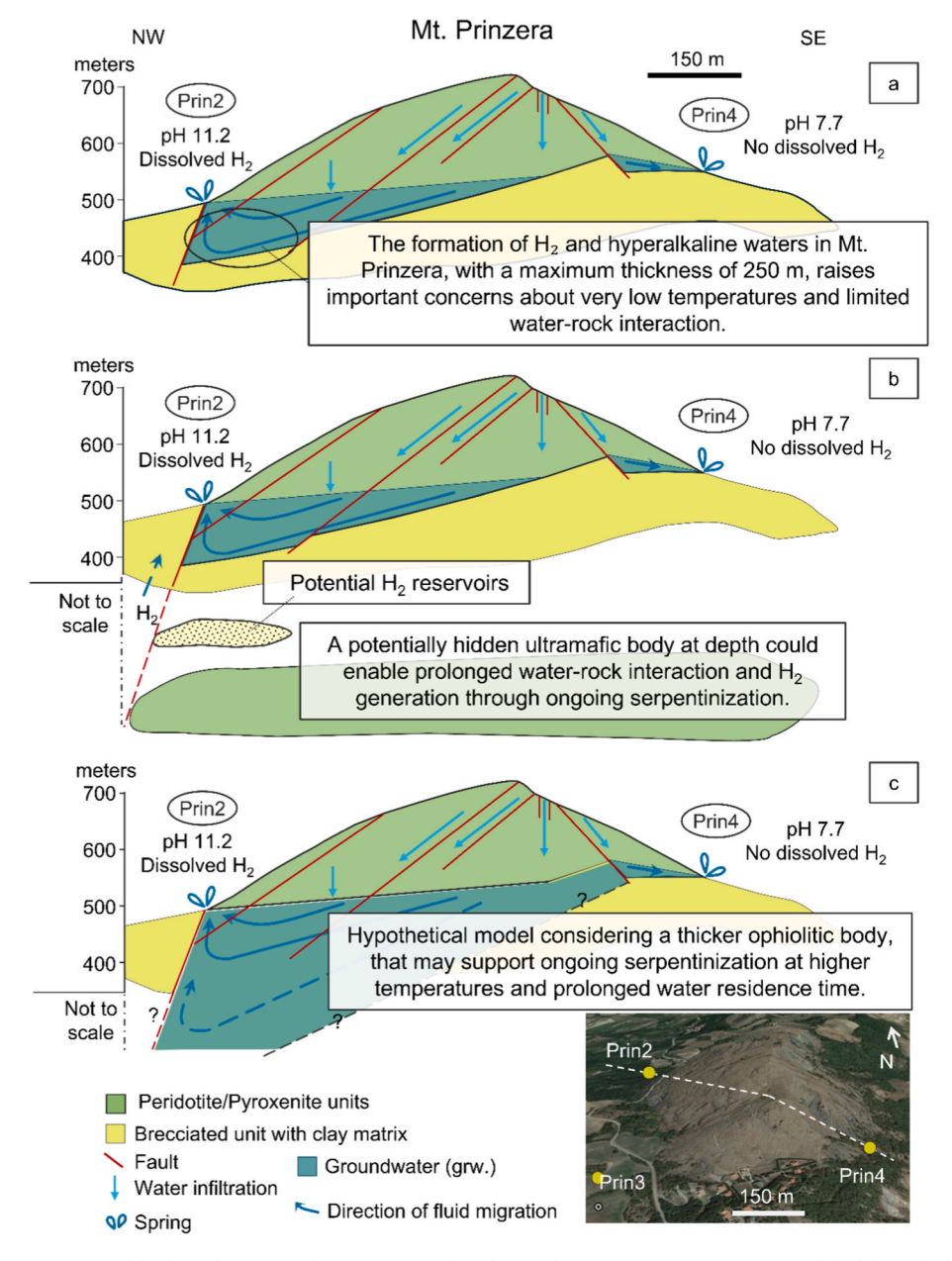


Fig. 5. Hypothetical H₂ generation models through water-rock interaction within the peridotite units in Mt. Prinzera (modified from the high-flow hydrogeological model proposed by Segadelli et al., 2017a). a) The H₂ generation model is based on water-rock interaction within the peridotite units in Mt. Prinzera, considering a maximum thickness of 250 m. b) The model considers the presence of a hidden ultramafic body beneath the boundaries of Mt. Prinzera, generating H₂ through ongoing serpentinization at greater depths. c) This model assumes a deeper root for the ultramafic body of Mt. Prinzera than previously estimated by (Segadelli et al., 2017a), allowing ongoing serpentinization and H₂ generation due to increased depth and temperature and considering a longer water residence time. Dashed lines indicate hypothetical traces. Satellite image from Google Earth Pro (2025), image date 9/18/2022. The vertical scale corresponds to meters above sea level (m.a.s.l.).

NaCl brine waters, such as those found in the Bobbio region, exhibit significantly lower H_2 solubility than pure water (Lopez-Lazaro et al., 2019).

 $\rm H_2$ in the bubbling gas at Bobbio has only been investigated using GC, with a detection limit of 400 ppmv. Further analyses should be conducted using more sensitive instruments.

The very low concentrations of H₂ observed in the soil cannot confirm a geological H₂ seepage, as these levels could be artificially generated during the drilling process or may result from microbial H₂ production in wet ground layers adjacent to the springs (Davies et al., 2025; Etiope and Orban, 2025). Nevertheless, it is important to emphasize that the soil-gas study conducted was preliminary to check H₂ occurrence around the selected springs. A more extensive soil-gas survey is needed, as previous studies reported significant spatial and temporal variability of H₂ values from soil-gas measurements (e.g., Zgonnik et al., 2015; Moretti et al., 2021b; Lévy et al., 2023; Loiseau et al., 2024). Soil-gas measurements, particularly along faults in the Prinzera and Bobbio areas, should be carried out to verify the existence of natural H₂ seepage potentially related to subsurface H₂-enriched accumulations.

5.2. Potential of H_2 generation in subsurface rocks

5.2.1. Sites associated with ophiolites

According to Segadelli et al. (2017a and b), brecciated and serpentinized peridotites in Mt. Prinzera, originally exhibiting very low permeability, are extensively fractured, resulting in significant vertical hydrogeological heterogeneity. Multiple deformation phases affected the entire massif. Notably, Quaternary extensional tectonic events resulted in high-angle faults predominantly oriented WNW-ESE. These structures control groundwater flow, with perennial springs primarily sustained by deep groundwater sources (Segadelli et al., 2017a; and b). In the western sector, within the hyperalkaline spring zone, groundwater is likely to circulate deeply and for extended periods along the fault network, emerging with high pH and with dissolved CH₄ and H₂ (Fig. 5a). In contrast, in the eastern part, the water flows over shorter and shallower paths, resulting in neutral pH and negligible CH₄ and H₂ content.

The presence of H₂, associated with a hyperalkaline spring within the ultramafic rock body at Mt. Prinzera, suggests that serpentinization is the main H₂-generating process. Nonetheless, possible maximum thickness of the Mt. Prinzera body, approximately 250 m, as estimated by Segadelli et al. (2017a), would imply very low-temperature serpentinization and would not be compatible with deep water circulation models required to form high pH waters (e.g., Barnes et al., 1972; Cipolli et al., 2004). At such shallow depths, the expected maximum temperature is approximately 30 °C, assuming an average regional geothermal gradient of 21.2 °C/km (Acosta et al., 2024) and a surface temperature of 25 °C. Several studies have demonstrated that oxido-reduction reactions can generate H₂ at low temperatures (below 150 °C, e.g., Geymond et al., 2023; Leong et al., 2023; Carlin et al., 2024; Templeton et al., 2024). Additionally, experimental models have demonstrated that H₂ can be produced from ultramafic protoliths even at very low temperatures (between 30 °C and 70 °C, Neubeck et al., 2011).

Even considering H₂ generation at such low temperatures plausible, the origin of the hyperalkaline water at Prin2 is still puzzling. Sodiumrich hyperalkaline waters, such as Prin2, require a relatively long residence time and deep circulation within a closed system for CO₂ to evolve from Mg-HCO₃ waters, like those found in the non-hyperalkaline springs in Prinzera (Barnes et al., 1972; Bruni et al., 2002; Cipolli et al., 2004). Based on geochemical thermodynamic modeling, prolonged water-rock interaction at depth for Prin2 is supported by Boschetti and Toscani (2008, which included Galla) and Segadelli et al. (2017a). However, none of these studies discussed how such prolonged residence time could occur within an ophiolitic body estimated to be only a few hundred meters thick.

Alternative models involving higher serpentinization temperatures, exceeding 50 $^{\circ}$ C, and longer residence pathways inside the ultramafic body can also be hypothesized. One model assumes the presence of a hidden ultramafic body beneath Mt. Prinzera, generating H₂-rich fluids through serpentinization at greater depths and longer residence time. These fluids could then ascend along faults, reaching potential reservoirs and the surface (Fig. 5b). The widespread presence of ultramafic slideblocks in the External Ligurian, especially in the study area, supports the possibility of ultramafic bodies under Mt. Prinzera. It can also be hypothesized that the thickness of the Mt. Prinzera body is greater than previously estimated. If this is the case, the base of the ultramafic body could extend deeper, providing longer water circulation and facilitating H_2 generating and the existence of hyperalkaline waters (Fig. 5c).

These speculative models (Fig. 5) require further investigation to understand the origin of the hyperalkaline waters at Prinzera and their associated hydrogen content.

Regardless of the hypothetical scenario, the mineral assemblage of peridotites may offer valuable insights into the temperature conditions during serpentinization. According to thermodynamic models and considering the general serpentinization reaction — Olivine $+ H_2O \rightarrow$ Serpentine + Brucite + Magnetite + H₂ — the formation of specific minerals varies depending on the protolith composition and temperature (Klein et al., 2013). The absence of brucite in petrographic studies is notable when considering low-temperature serpentinization as the mechanism for H2 generation at Mt. Prinzera since brucite typically forms during the serpentinization of olivine at low temperatures. However, its formation is not predicted in models where at least 50 % of pyroxene undergoes serpentinization along with olivine (Klein et al., 2013), which is the case at Mt. Prinzera (Fig. 3). Magnetite formation during serpentinization is generally associated with temperatures exceeding 200 °C (Klein et al., 2013), but minor amounts may still form at lower temperatures (Klein et al., 2020). Thus, the small amounts of magnetite observed in a few thin sections of Mt. Prinzera peridotites align with low-temperature serpentinization. Considering the serpentinization of olivine Fo₈₉ (Montanini et al., 2006) at low temperatures (<200 °C), thermodynamic models predict limited H₂ production, below 200 mmol/kg (Klein et al., 2013), which could explain the low H₂ concentration measured at Mt. Prinzera. However, the petrographic studies alone were not conclusive in constraining the serpentinization conditions. Additional mineral and rock studies should be carried out on the peridotite rocks to investigate the possible serpentinization at Mt. Prinzera properly.

It is noteworthy that, despite its relatively low concentrations, $\rm H_2$ has been consistently detected at the Prin2 spring over multiple years (2011, 2019, and 2023) and during both summer and winter. This constant detection suggests the presence of a persistent migration of $\rm H_2$, likely from underground $\rm H_2$ -rich aquifers or reservoirs or prolific generating rocks crossed by the hyperalkaline waters. The variation in dissolved $\rm H_2$ concentrations over time indicates that $\rm H_2$ input into the groundwater changes, possibly due to variable groundwater flow pathways and/or interaction with $\rm H_2$ - bearing rock, and/or biotic or abiotic $\rm H_2$ consumption.

Notably, the Prin3 spring, located in the southwestern part of the massif (Figs. 1 and 5, satellite image), has neutral pH and low CH $_4$ levels, but exhibits dissolved H $_2$ concentrations similar to those of the hyperalkaline springs. The presence of H $_2$ in Prin3 may result from mixing deeper water, related to the serpentinization process with shallower recharge waters.

At Galla (Fig. 1a), no previous studies have been carried out to evaluate hydrogeological aspects. However, the presence of hyperalkaline water suggests favorable water-rock interaction under appropriate conditions that may have generated H_2 . Nevertheless, CH_4 concentrations are significantly lower than those at Mt. Prinzera, likely due to the reduced potential for thermogenic methane generation in the sedimentary rocks of the region.

In the hyperalkaline Issel Spring (Fig. 1b), the concentration of

dissolved $\rm H_2$ below the detection limit suggests that the serpentinization process in the subsurface, evidenced by the high pH, is incapable of producing $\rm H_2$ in detectable quantities or that biotic or abiotic processes totally consume any produced $\rm H_2$. The limited $\rm H_2$ production during the serpentinization may be due to insufficient water supply or circulation within the ultramafic massif, which can reduce the water/rock ratio and fails to provide the necessary conditions for $\rm H_2$ generation. Moreover, the absence of dissolved $\rm H_2$ in other springs associated with ultramafic bodies, such as Mt. Sant'Agostino, Mt. Zirone, Rocca Galgana, and Mogge Alta (Fig. 1a and c), aligns with their approximately neutral pH, suggesting that no active serpentinization is taking place in the subsurface.

5.2.2. Sites lacking exposed ultramafic rocks

The notable concentration of dissolved H_2 in the Bobbio Tectonic Window (3.86 μ M in Bobbio3 spring, Table 1) represents the highest measured value in the western sector of Northern Apennines and was unexpected, as the water is not hyperalkaline. The measured concentration (Table 1) is one order of magnitude higher than the level attributed to microbial processes (0.426 μ M; Etiope and Orban, 2025, Table 1). Additionally, it is comparable to levels observed in hyperalkaline springs associated with ultramafic bodies like the Ronda Peridotite in Spain and Voltri in Italy (Fig. 4a). Thus, there may be a geological source of H_2 within the Bobbio Structural Window. Thrust faults related to the Apenninic Belt, along with younger normal faults, both predominantly NW-SE oriented, may act as migration pathways. These structural features could connect deep H_2 generation sites to the surface, even at considerable depth.

The chloride-rich fossil marine waters in the Bobbio area (Duchi et al., 2005; Boschetti et al., 2011) exhibit neutral pH and do not seem to have passed through active serpentinization zones, as might occur in Mt. Prinzera. Consequently, H_2 generation does not appear to be associated with this relatively shallow process, especially considering the absence of ultramafic outcrops nearby. An alternative process may, therefore, be responsible for H_2 generation within the subsurface.

The isotopic composition of CH₄ can provide insights into the process occurring in the subsurface. The $\delta^2 H_{CH4}$, $\delta^{13} C_{CH4}$ and $\delta^{13} C_{CO2}$ values

suggest a thermogenic origin for the dissolved methane in the Bobbio1 and Bobbio2 springs, as well as for the free gas from Bobbio4 (Fig. 6). These results are consistent with the broader classification of light hydrocarbons in the western part of the Northern Apennines (Borgia et al., 1988; Duchi et al., 2005; Martinelli et al., 2012). The dissolved methanes in Bobbio3 and Bobbio4 are enriched in both deuterium and ${}^{13}\mathrm{C}$ relative to the other springs (Fig. 6a), suggesting methane oxidation near the surface. Coleman et al. (1981) reported isotopic enrichment of δ^2 H and δ^{13} C in experiments on microbial methane oxidation. They observed a variation in δ^2 H (Δ H) relative to δ^{13} C (Δ C), with the Δ H/ Δ C ratio ranging from 8 to 14 times higher depending on the temperature. The lowest $\Delta H/\Delta C$ ratio was noted at approximately 11.5 °C, while the highest ratio occurred near 26 $^{\circ}$ C. The data from Bobbio3 and Bobbio4 show a $\Delta H/\Delta C$ ratio of approximately 10.3, suggesting microbial oxidation of thermogenic gas, whose original isotopic signature is maintained in other Bobbio springs (Bobbio1 and Bobbio2; Fig. 6a). Regarding a possible abiotic origin of methane, although dissolved H₂ is present, which could contribute to Fischer-Tropsch-type reactions, the isotopic data of methane does not provide clear evidence for an abiotic origin. However, the combination of $\delta^{13}C_{CH4}$ and $\delta^{13}C_{CO2}$ does not clearly distinguish between abiotic and thermogenic origin (Fig. 6b). Therefore, a minor abiotic contribution cannot be ruled out.

A potential origin of $\rm H_2$ in the Bobbio zone through serpentinization of ultramafic rocks can be hypothesized, even within a structural window dominated by sedimentary rocks. The complex tectonic setting of the Northern Apennines, marked by imbricated thrust stacks, allows the presence of ophiolitic slices from the Ligurian Unit intercalated with the sedimentary succession of Tuscan units. This structural configuration was confirmed during drilling of the Pontremoli well, located 55 km to the southeast of Bobbio, where the Subligurian and Ligurian units were encountered beneath the Tuscan units at depths >1 km (Agip, 1971, 1971; Artoni et al., 1992). The neutral pH, chloride-rich waters could be responsible for transporting $\rm H_2$ in dissolved form. In this scenario, $\rm H_2$ could have been generated through serpentinization at greater depths, possibly in the past, with the gas trapped in reservoirs. Over time, the trapped $\rm H_2$ could have migrated along deep-seated faults toward the surface, eventually released and dissolved in water. $\rm H_2$ as free gas could

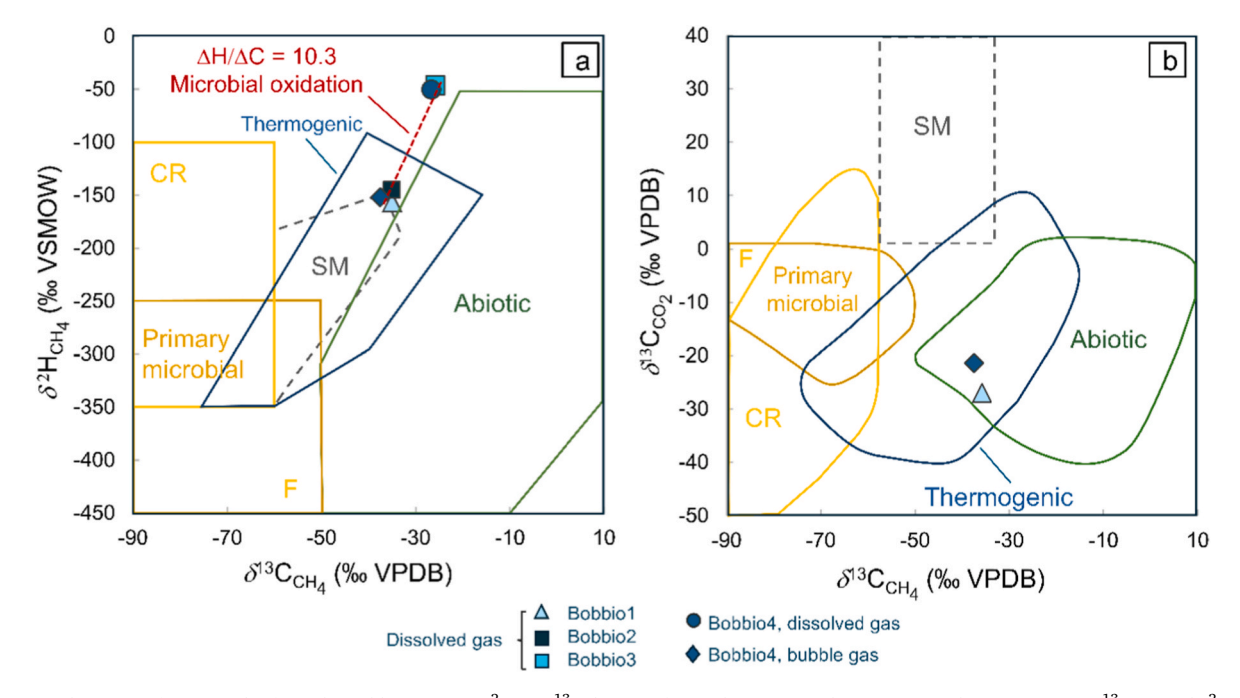


Fig. 6. Genetic diagrams of gas samples from the Bobbio zone. a) $\delta^2 H$ vs. $\delta^{13} C$ diagram for methane. ΔH and ΔC represent the variations in $\delta^{13} C_{CH4}$ and $\delta^2 H_{CH4}$ values during methane oxidation. The slope of the dashed red line (10.3) suggests that microbial oxidation could be active in the Bobbio3 and Bobbio4 springs. b) $\delta^{13} C_{CO2}$ vs. $\delta^{13} C_{CH4}$ diagram. Genetic fields were reported by Milkov and Etiope (2018). Notations: $CR - CO_2$ reduction, F – fermentation, and SM - secondary microbial. (For interpretation of the references to colour in this figure legend, the reader is referred to the Web version of this article.)

also be present, but our preliminary studies did not detect it. Additional dedicated studies are required to explore these hypotheses further.

Besides Fe-rich rocks as a source of $\rm H_2$, active large fault zones may not only serve as pathways for $\rm H_2$ migration from deep sources but could also drive $\rm H_2$ generation processes via mechanoradical fracture-induced reduction of water (Zgonnik, 2020 and references therein). This $\rm H_2$ generation mechanism has not been fully tested. In the Bobbio area, however, deep-seated faults may serve as pathways for $\rm H_2$ migration from deep sources but are unlikely to generate $\rm H_2$ through a mechanoradical process, as no active faults occur in the region (DISS Working Group, 2021). Additionally, a thermogenic origin of $\rm H_2$ from overmature organic matter cannot be ruled out. The presence of nearby natural gas fields confirms that organic matter has reached thermal maturity, and further maturation beyond the gas window at higher temperatures could also lead to $\rm H_2$ generation (Horsfield et al., 2022; Boreham et al., 2023).

The spring Bobbio2, although situated in the same area, has dissolved $\rm H_2$ below the detection limit. The cause of this phenomenon remains unclear, but it may be attributed to either biotic or abiotic $\rm H_2$ consumption or potentially inefficient migration pathways. The higher dissolved $\rm CH_4$ concentration could suggest that $\rm H_2$ has been consumed during $\rm CH_4$ formation through Fischer-Tropsch type reactions. Nevertheless, the $\delta^2\rm H$ and $\delta^{13}\rm C$ isotopic values for methane do not support an abiotic source for methane.

5.3. Hypothesis for a natural H_2 system and its exploration

The results of this study suggest that a potentially natural $\rm H_2$ system may exist in the External Ligurian ophiolites (Mt. Prinzera and Groppo di Gorro) and in the Bobbio Tectonic Window. Table 5 summarizes elements of the potential natural $\rm H_2$ systems in the Mt. Prinzera and Bobbio areas.

In ophiolite-related areas, low concentrations of dissolved $\rm H_2$ in water reduce the potential for direct $\rm H_2$ exploitation. However, reservoir rocks are present in the Taro Valley region. Hydrocarbon reservoirs have been exploited since the early 20th century, including the now-inactive Vallezza oil field and currently active natural gas concessions of Fornovo di Taro and Monte Ardone, located approximately 5 km northeast of Mt. Prinzera. The occurrence of porous rocks in the region suggests the potential presence of $\rm H_2$ -bearing reservoirs in the Mt. Prinzera area, as illustrated in Fig. 5b.

An emerging technique known as geological hydrogen stimulation could also enable future H₂ exploitation at ultramafic bodies. This technique focuses on hydraulic and chemical stimulation of iron-rich rocks to increase the rate of H₂ generation while also controlling the temperature, biological activity, and fluids production (Osselin et al., 2022). Ongoing studies are assessing the feasibility of this method, with notable projects in Oman (Templeton et al., 2024) and the United States. If validated, these engineered water/rock reactions could provide an application in ultramafic massifs like those in the Northern Apennines. However, the potential success of these methods also depends on factors such as the size of each ultramafic body and the proportion of fresh peridotite, which would determine whether there is sufficient rock

volume to support significant H₂ production.

The potential of geological H_2 generation within the Bobbio Tectonic Window represents an interesting case study from a scientific perspective since it is not associated with active serpentinization of outcropping ultramafic bodies. From an economic perspective, the H_2 occurrences identified in this study do not indicate a significant surface H_2 flux, particularly in terms of free gas. However, the area holds the potential to contain key elements of a natural hydrogen system, such as generation rocks, reservoirs, seals, and traps.

The region of Bobbio may host reservoirs in several geological units, such as Miocene turbiditic foredeep deposits and Triassic dolomites, which were previously targeted by the oil and gas industry in nearby areas (Coparex International, 1989; Agip, 1990; Eni, 2003). Furthermore, an active oil and gas production field named Pigazzano is located 15 km northeast. Although these reservoirs have not been previously tested for H₂, they could potentially host this gas, particularly considering H₂ generation at greater depths in the Bobbio Tectonic Window.

Finally, it is important to highlight that natural hydrogen exploration is currently unregulated in Italy. Discussions on establishing a dedicated regulatory framework, similar to initiatives underway in other countries, are essential to foster this potentially emerging sector in Italy.

6. Conclusions

This study demonstrates the presence of dissolved $\rm H_2$ of likely geological origin at two sites in the Northern Apennines: hyperalkaline spring regions associated with the External Ligurian ophiolites (Mt. Prinzera and Groppo di Gorro) and the Bobbio Tectonic Window, respectively at the foothills and hinterland of the Northern Apennines orogenic wedge. Conversely, no $\rm H_2$ was detected in the Internal Ligurian ophiolites (Castagnola area) or neutral pH springs linked to ultramafic rocks of External Ligurian (Mt. Sant'Agostino, Mt. Zirone, and Rocca Galgana). An exception is the neutral pH spring Prin3 at Mt. Prinzera, located relatively close to the hyperalkaline spring, where $\rm H_2$ has also been detected. No appreciable $\rm H_2$ seepage in the soil was detected in the surroundings of the investigated springs.

In the ophiolitic massifs of Mt. Prinzera and Groppo di Gorro, the interaction of groundwater with ultramafic rocks is likely responsible for the observed dissolved $\rm H_2$. Petrographic studies reveal peridotites with varying degrees of serpentinization (45 %–100 %), with original olivine and ortho-/clinopyroxenes replaced by serpentine, which also occurs in veins with magnetite. However, the estimated limited thickness of the Mt. Prinzera (~250 m) appears insufficient to produce hyperalkaline water and provides the optimal conditions for $\rm H_2$ generation via serpentinization. This thickness limitation suggests that the hyperalkaline water and $\rm H_2$ origin may instead be linked to deeper-seated peridotite bodies undergoing serpentinization. Notably, while $\rm H_2$ concentrations at Mt. Prinzera were relatively low compared to other hyperalkaline waters associated with ultramafic units, they have remained constant over the years.

Although the Bobbio Tectonic Window lacks exposed ophiolitic outcrops, it still shows low to intermediate concentrations of dissolved

Table 5Presence of key elements of the natural H₂ system for the initial stage of hydrogen exploration at Mt. Prinzera and the Bobbio Tectonic Window, where the studies are primarily focused.

Site	H ₂ indicators	Generation Rocks/Process	Migration Pathways and traps	Accumulation in subsurface	
Mt. Prinzera	Yes	Yes	Possible	Possible	
	Low concentrations of dissolved (likely) geological H ₂	$\rm H_2$ generation probably via serpentinization. Peridotite and serpentinite outcrops.	Apenninic thrusts and locally normal faults	Porous rocks confirmed in nearby areas (presence of oil and gas accumulations)	
Bobbio	Yes	Yes	Possible	Possible	
Tectonic Window	Low to intermediate levels of dissolved geological H ₂ .	$\rm H_2$ generation origin still uncertain. Probably serpentinization of hidden ultramafic rocks.	Apenninic thrusts and locally normal faults	Porous rocks confirmed in nearby areas (presence of gas accumulations)	

H₂, likely of geological origin. A plausible explanation is the potential presence of hidden ultramafic bodies of the Ligurian units hosted within the sedimentary rocks of the Tuscan units.

Further studies may involve the interpretation of available geophysical surveys (e.g., seismic reflection, gravimetric and magnetic surveys) to investigate potential accumulation targets and generation rocks at depth, as well as additional petrographic and geochemical analyses of rocks and minerals to assess the $\rm H_2$ generation potential of the outcropping ultramafic rocks.

CRediT authorship contribution statement

Vivian Azor de Freitas: Writing – review & editing, Writing – original draft, Visualization, Methodology, Investigation, Formal analysis, Data curation, Conceptualization. Alessandra Montanini: Writing – review & editing, Investigation, Funding acquisition. Isabelle Moretti: Writing – review & editing, Resources, Conceptualization. Andrea Artoni: Writing – review & editing. Stefano Segadelli: Writing – review & editing, Investigation. Jean de la Paix Izerumugaba: Writing – review & editing, Resources, Investigation. Giuseppe Etiope: Writing – review & editing, Validation, Resources, Methodology, Investigation, Funding acquisition, Formal analysis.

Funding sources

This study was supported by the COMP-R Initiative, funded by the "Departments of Excellence" program of the Italian Ministry for University and Research (MUR, 2023–2027), the Cariparma Foundation (grant 2023-0606), and European Union – NextGenerationEU and the Romanian Government (National Recovery and Resilience Plan for Romania, contract no 760039/May 23, 2023, cod PNRR-C9-I8-CF 14/November 11, 2022).

Declaration of competing interest

The authors declare that they have no known competing financial interests or personal relationships that could have appeared to influence the work reported in this paper.

Acknowledgments

This research was financially supported by the COMP-R Initiative, funded by the "Departments of Excellence" program of the Italian Ministry for University and Research (MUR, 2023–2027) and the Cariparma Foundation (grant 2023-0606). We are grateful for the dissolved hydrogen and CRDS analyses at the ENGAGE laboratory (Babes Bolyai University, Cluj-Napoca), funded by European Union – NextGenerationEU and the Romanian Government (National Recovery and Resilience Plan for Romania, contract no 760039/May 23, 2023, cod PNRR-C9-I8-CF 14/November 11, 2022). We thank Gianpiero Brozzo (Iren), Mario Polledri (Ireti), Eleonora Valentini, and Fernanda Rabello de Oliveira for their help with water/gas sampling and fieldwork. We are grateful to Roberto Tinterri for supporting and making this work possible. We also thank Kenneth Peters, Pawel Kosakowski, and the anonymous reviewers for their valuable and constructive contributions, which improved the quality of the manuscript.

Data availability

Data will be made available on request.

References

Acosta, D.B., Toscani, G., Colombera, L., Amadori, C., Fantoni, R., Di Giulio, A., 2024.

Predicting the thermal regime of the Po plain subsurface (italy) using geostatistical

- modeling constrained by legacy wells. Mar. Petrol. Geol. 167, 106936. https://doi.
- Agip, S.p.a., 1971. Final geologic report of Pontremoli 1 well. Available online: http s://www.videpi.com/deposito/pozzi/profili/pdf/pontremoli_001.pdf. (Accessed 4 October 2025).
- Agip, S.p.a., 1990. Relazione tecnica allegata all'istanza di rinuncia del permesso di ricercar di idrocarburo liquidi e gassosi "Caldirola" (Technical report related to relinquish the exploration permit for liquid and gaseous hydrocarbons "Cardirola"). Available online: https://www.videpi.com/videpi/cessati/fascicolo.asp?titolo=157, 03/27/2025.
- Aiuppa, A., Moussallam, Y., 2024. Hydrogen and hydrogen sulphide in volcanic gases: abundance, processes, and atmospheric fluxes. Comptes rendus. Geoscience 356 (S1), 1–23. Iyhttps://doi.org/10.5802/crgeos.235.
- Artoni, A., Bernini, M., Papani, G., Vescovi, P., Zanzucchi, G., 1992. Sezione geologica schematica Bonassola (SP)-Felino (PR). Stud. Geol. Camerti 2, 61–63. http://193.2 04.8.201:8080/jspui/handle/1336/413.
- Barnes, I., Rapp, J.B., O'Neil, J.R., Sheppard, R.A., Gude, A.J., 1972. Metamorphic assemblages and the direction of flow of metamorphic fluids in four instances of serpentinization. Contrib. Mineral. Petrol. 35, 263e276. https://doi.org/10.1007/ BEOGA 122
- Beltrando, M., Stockli, D.F., Decarlis, A., Manatschal, G., 2015. A crustal-scale view at rift localization along the fossil Adriatic margin of the Alpine Tethys preserved in NW Italy. Tectonics 34, 1927–1951. https://doi.org/10.1002/2015TC003973.
- Boreham, C.J., Edwards, D.S., Czado, K., Rollet, N., Wang, L., van der Wielen, S., et al., 2021. Hydrogen in Australian natural gas: occurrences, sources and resources. APPEA Journal 61 (1), 163–191. https://doi.org/10.1071/AJ20044.
- Boreham, C.J., Edwards, D.S., Feitz, A.J., Murray, A.P., Mahlstedt, N., Horsfield, B., 2023. Modelling of hydrogen gas generation from overmature organic matter in the Cooper Basin, Australia. APPEA Journal 63 (2), S351–S356. https://doi.org/ 10.1071/AJ22084.
- Borgia, G.C., Elmi, C., Ricchiuto, T., 1988. Correlation by genetic properties of the shallow gas seepages in the Emilian Apennine (Northern Italy). In: Organic Geochemistry in Petroleum Exploration. Pergamon, pp. 319–324. https://doi.org/ 10.1016/0146-6380(88)90051-4.
- Boschetti, T., Toscani, L., 2008. Springs and streams of the Taro–Ceno Valleys (Northern Apennine, Italy): reaction path modeling of waters interacting with serpentinized ultramafic rocks. Chem. Geol. 257, 76–91. https://doi.org/10.1016/j. chemgeo.2008.08.017.
- Boschetti, T., Toscani, L., Shouakar-Stash, O., Iacumin, P., Venturelli, G., Mucchino, C., Frape, S.K., 2011. Salt waters of the Northern Apennine Foredeep Basin (Italy): origin and evolution. Aquat. Geochem. 17, 71–108. https://doi.org/10.1007/s10498-010-9107-y.
- Boschetti, T., Etiope, G., Pennisi, M., Romain, M., Toscani, L., 2013. Boron, lithium and methane isotope composition of hyperalkaline waters (Northern Apennines, Italy): terrestrial serpentinization or mixing with brine? Appl. Geochem. 32, 17–25. https://doi.org/10.1016/j.apgeochem.2012.08.018.
- Boulart, C., Chavagnac, V., Monnin, C., Delacour, A., Ceuleneer, G., Hoareau, G., 2013. Differences in gas venting from ultramafic-hosted warm springs: the example of Oman and Voltri ophiolites. Ofioliti 38 (2), 143–156. https://doi.org/10.4454/ ofioliti.v38i2.423.
- Brass, M., Röckmann, T., 2010. Continuous-flow isotope ratio mass spectrometry method for carbon and hydrogen isotope measurements on atmospheric methane. Atmos. Meas. Tech. 3 (6), 1707–1721. https://doi.org/10.5194/amt-3-1707-2010.
- Brazelton, W.J., Thornton, C.N., Hyer, A., Twing, K.I., Longino, A.A., Lang, S.Q.,
 Lilley, M.D., Früh-Green, G.L., Schrenk, M.O., 2017. Metagenomic identification of
 active methanogens and methanotrophs in serpentinite springs of the Voltri Massif,
 Italy. PeerJ 5, e2945. https://doi.org/10.7717/peerj.2945.
 Bruni, J., Canepa, M., Chiodini, G., Cioni, R., Cipolli, F., Longinelli, A., Marini, L.,
- Bruni, J., Canepa, M., Chiodini, G., Cioni, R., Cipolli, F., Longinelli, A., Marini, L., Ottonello, G., Zuccolini, M.V., 2002. Irreversible water–rock mass transfer accompanying the generation of the neutral, Mg–HCO₃ and high-pH, Ca–OH spring waters of the Genova province, Italy. Appl. Geochem. 17 (4), 455–474. https://doi.org/10.1016/S0883-2927(01)00113-5.
- Capasso, G., Inguaggiato, S., 1998. A simple method for the determination of dissolved gases in natural waters. An application to thermal waters from Vulcano Island. Appl. Geochem. 13, 631–642. https://doi.org/10.1016/S0883-2927(97)00109-1.
- Cardace, D., Meyer-Dombard, D.A.R., Woycheese, K.M., Arcilla, C.A., 2015. Feasible metabolisms in high pH springs of the Philippines. Front. Microbiol. 6, 10. https://doi.org/10.3389/fmicb.2015.00010.
- Carlin, W., Malvoisin, B., Brunet, F., Lanson, B., Findling, N., Lanson, M., et al., 2024. Kinetics of low-temperature H₂ production in ultramafic rocks by ferroan brucite oxidation. Geochemical Perspectives Letters 29, 27–32. https://doi.org/10.7185/ geochemlet.2408.
- Cipolli, F., Gambardella, B., Marini, L., Ottonello, G., Vetuschi Zuccolini, M., 2004. Geochemistry of high-pH waters from serpentinites of the Gruppo di Voltri (Genova, Italy) and reaction path modelling of CO₂ sequestration in serpentinite aquifers. Appl. Geochem. 19, 787–802. https://doi.org/10.1016/j.apgeochem.2003.10.007.
- Coleman, D.D., Risatti, J.B., Schoell, M., 1981. Fractionation of carbon and hydrogen isotopes by methane-oxidizing bacteria. Geochem. Cosmochim. Acta 45 (7), 1033–1037. https://doi.org/10.1016/0016-7037(81)90129-0.
- Conti, P., Cornamusini, G., Carmignani, L., 2020. An outline of the geology of the Northern Apennines (Italy), with geological map at 1: 250,000 scale. Italian Journal of Geosciences 139 (2), 149–194. https://doi.org/10.3301/IJG.2019.25.
- Cook, M.C., Blank, J.G., Rietze, A., Suzuki, S., Nealson, K.H., Morrill, P.L., 2021. A geochemical comparison of three terrestrial sites of Serpentinization: the tablelands, the cedars, and aqua de Ney. J. Geophys. Res.: Biogeosciences 126 (11), e2021JG006316. https://doi.org/10.1029/2021JG006316.

- Coparex International, 1989. Relazione tecnica dei lavori eseguiti durante il primo, il secondo e parte del terzo period di vigenza del permesso di ricerca idrocarburi "Romagnese" allegata all'istanza di rinuncia (Technical report on the activities carried out during the first, second, and part of the third validity period of the "Romagnese" hydrocarbon exploration permit, submitted in support of the relinquishment application). Available online: https://www.videpi.com/videpi/cessati/fascicolo.asp?titolo=717, 03/27/2025.
- D'Alessandro, W., Daskalopoulou, K., Calabrese, S., Bellomo, S., 2018. Water chemistry and abiogenic methane content of a hyperalkaline spring related to serpentinization in the Argolida ophiolite (Ermioni, Greece). Mar. Petrol. Geol. 89, 185–193. https:// doi.org/10.1016/j.marpetgeo.2017.01.028.
- Davies, K., Josse, R., Frery, E., Esteban, L., Keshavarz, A., Iglauer, S., 2025. Distinguishing drilling-induced artifacts from naturally occurring hydrogen in soil gas surveys: insights from sub-circular depressions. Int. J. Hydrogen Energy 109, 1230–1240. https://doi.org/10.1016/j.ijhydene.2025.02.094.
- DISS Working Group, 2021. Database of Individual Seismogenic Sources (DISS), version 3.3.0: a compilation of potential sources for earthquakes larger than M 5.5 in Italy and surrounding areas. Istituto Nazionale. https://doi.org/10.13127/diss3.3.0.
- Duchi, V., Venturelli, G., Boccasavia, I., Bonicolini, F., Ferrari, C., Poli, D., 2005. Studio geochimico dei fluidi dell'Appennino Tosco-Emiliano-Romagnolo (Geochemical study of the fluids of the Tuscan-Emilian-Romagnolo Apennines). Boll. Soc. Geol. Ital. 124 (2), 475–491. Available online: https://pubs.geoscienceworld.org/sgi/italianjgeo/article/124/2/475/74931/Studio-geochimico-dei-fluidi-dell-Appennino-To sco. (Accessed 4 November 2025).
- Dugamin, E., Truche, L., Donze, F.V., 2019. Natural Hydrogen Exploration Guide, vol. 1. ISRN Geonum-NST, p. 16.
- Emilia-Romagna, Regione, 2016. Acque dalle rocce, una ricchezza della montagna: percorsi interdisciplinari nell'affascinante mondo delle sorgenti. Servizio Geologico, Sismico e dei Suoli. Regione Emilia-Romagna (Water from the rocks, a treasure of the mountains: interdisciplinary journeys into the fascinating world of springs. Geological, Seismic and Soil Service, Emilia-Romagna Region). Available online: htt ps://ambiente.regione.emilia-romagna.it/it/geologia/divulgazione/pubblicazioni/libri/acque-dalle-rocce-una-ricchezza-della-montagna-2016, 04/01/2025.
- Eni, S.p.a., 2003. Permesso Torrente Luretta, relazione tecnica allegata all'istanza di rinuncia del titolo (Torrente Luretta permit, technical report submitted in support of the relinquishment application). Available online: https://www.videpi.com/vide pi/cessati/relazione.asp?titolo=848&relazione=2200, 03/27/2025.
- Etiope, G., Orban, A., 2025. Surface gas geochemical exploration for natural hydrogen: uncertainties and holistic interpretation. In: Rezaee, R., Evans, B. (Eds.), Natural Hydrogen Systems: Properties, Occurrences, Generation Mechanisms, Exploration, Storage, and Transportation. De Gruyter Academic Publishing, Berlin, pp. 347–365. https://doi.org/10.1515/9783111437040-012.
- Etiope, G., Whiticar, M.J., 2019. Abiotic methane in continental ultramafic rock systems: towards a genetic model. Appl. Geochem. 102, 139–152. https://doi.org/10.1016/j. apgeochem.2019.01.012.
- Etiope, G., Caracausi, A., Favara, R., Italiano, F., Baciu, C., 2002. Methane emission from the mud volcanoes of Sicily (Italy). Geoph. Res. Lett. 29, 8. https://doi.org/10.1029/ 2001GL014340.
- Etiope, G., Tsikouras, B., Kordella, S., Ifandi, E., Christodoulou, D., Papatheodorou, G., 2013. Methane flux and origin in the Othrys ophiolite hyperalkaline springs, Greece. Chem. Geol. 347, 161–174. https://doi.org/10.1016/j.chemgeo.2013.04.003.
- Etiope, G., Vadillo, I., Whiticar, M.J., Marques, J.M., Carreira, P.M., Tiago, I., Benavente, J., Jimenez, P., Urresti, B., 2016. Abiotic methane seepage in the Ronda peridotite massif, southern Spain. Appl. Geochem. 66, 101–113. https://doi.org/ 10.1016/j.apgeochem.2015.12.001.
- Etiope, G., Samardžić, N., Grassa, F., Hrvatović, H., Miošić, N., Skopljak, F., 2017. Methane and hydrogen in hyperalkaline groundwaters of the serpentinized Dinaride ophiolite belt, Bosnia and Herzegovina. Appl. Geochem. 84, 286–296. https://doi. org/10.1016/j.apgeochem.2017.07.006.
- Etiope, G., Ciotoli, G., Benà, E., Mazzoli, C., Röckmann, T., Sivan, M., et al., 2024. Surprising concentrations of hydrogen and non-geological methane and carbon dioxide in the soil. Sci. Total Environ. 948, 174890. https://doi.org/10.1016/j. scitoteny.2024.174890
- Fantoni, D., Brozzo, G., Canepa, M., Cipolli, F., Marini, L., Ottonello, G., Zuccolini, M., 2002. Natural hexavalent chromium in groundwaters interacting with ophiolitic rocks. Environ. Geol. 42, 871–882. https://doi.org/10.1007/s00254-002-0605-0.
- Feldbusch, E., Wiersberg, T., Zimmer, M., Regenspurg, S., 2018. Origin of gases from the geothermal reservoir Groß Schönebeck (North German Basin). Geothermics 71, 357–368. https://doi.org/10.1016/j.geothermics.2017.09.007.
- Ferrari, E., Montanini, A., Tribuzio, R., 2022. Rifting evolution of the lithospheric subcontinental mantle: new insights from the External Ligurian ophiolites (Northern Apennine, Italy). Lithos 410, 106571. https://doi.org/10.1016/j. lithos.2021.106571.
- Franceschelli, M., Gianelli, G., Pandeli, E., Puxeddu, M., 2004. Variscan and Alpine metamorphic events in the northern Apennines (Italy): a review. Period. Mineral. 73,
- Freitas, V.A., Prinzhofer, A., Françolin, J.B., Ferreira, F.J.F., Moretti, I., 2024. Natural hydrogen system evaluation in the S\(\tilde{a}\) o Francisco Basin (Brazil). Science and Technology for Energy Transition 79, 95. https://doi.org/10.2516/stet/2024091.
- Geologico d'Italia, Servizio, 2005. Carta geologica D'Italia Alla Scala 1:50.000, F. 199 Parma Sud. ISPRA. https://doi.org/10.15161/oar.it/150114.
- Geymond, U., Briolet, T., Combaudon, V., Sissmann, O., Martinez, I., Duttine, M., Moretti, I., 2023. Reassessing the role of magnetite during natural hydrogen generation. Front. Earth Sci. 11, 1169356. https://doi.org/10.3389/ feart.2023.1169356.

- Guélard, J., Beaumont, V., Rouchon, V., Guyot, F., Pillot, D., Jézéquel, D., et al., 2017.
 Natural H₂ in Kansas: deep or shallow origin? G-cubed 18 (5), 1841–1865. https://doi.org/10.1002/2016GC006544.
- Hao, Y., Pang, Z., Tian, J., Wang, Y., Li, Z., Li, L., Xing, L., 2020. Origin and evolution of hydrogen-rich gas discharges from a hot spring in the eastern coastal area of China. Chem. Geol. 538, 119477. https://doi.org/10.1016/j.chemgeo.2020.119477.
- Horsfield, B., Mahlstedt, N., Weniger, P., Misch, D., Vranjes-Wessely, S., Han, S., Wang, C., 2022. Molecular hydrogen from organic sources in the deep Songliao Basin, PR China. Int. J. Hydrogen Energy 47 (38), 16750–16774. https://doi.org/10.1016/j.ijhydene.2022.02.208.
- IEA, 2024. Global Hydrogen Review 2024. International Energy Agency (IEA). Available online: https://iea.blob.core.windows.net/assets/89c1e382-dc59-46ca-aa47-9f7d 41531ab5/GlobalHydrogenReview2024.pdf. (Accessed 4 November 2025).
- Klein, F., Bach, W., McCollom, T.M., 2013. Compositional controls on hydrogen generation during serpentinization of ultramafic rocks. Lithos 178, 55–69. https:// doi.org/10.1016/j.lithos.2013.03.008.
- Klein, F., Tarnas, J.D., Bach, W., 2020. Abiotic sources of molecular hydrogen on Earth. Elements: An International Magazine of Mineralogy, Geochemistry, and Petrology 16 (1), 19–24. https://doi.org/10.2138/gselements.16.1.19.
- Labaume, P., 2011. Carta geologica Dell'Appennino Emiliano-Romagnolo 1:10.000, Sezione 197010 Bobbio; Regione Emilia-Romagna, SELCA Stampe: Florence, Italy.
- Lefeuvre, N., Truche, L., Donzé, F.V., Gal, F., Tremosa, J., Fakoury, R.A., et al., 2022. Natural hydrogen migration along thrust faults in foothill basins: the North Pyrenean Frontal Thrust case study. Appl. Geochem. 145, 105396. https://doi.org/10.1016/j.appgochem.2022.105396
- Leila, M., Lévy, D., Battani, A., Piccardi, L., Šegvić, B., Badurina, L., Pasquet, G., Combaudon, V., Moretti, I., 2021. Origin of continuous hydrogen flux in gas manifestations at the Larderello geothermal field, Central Italy. Chem. Geol. 585, 120564. https://doi.org/10.1016/j.chemgeo.2021.120564.
- Leong, J.A., Nielsen, M., McQueen, N., Karolyte, R., Hillegonds, D.J., Ballentine, C., et al., 2023. H₂ and CH₄ outgassing rates in the Samail ophiolite, Oman: implications for low-temperature, continental serpentinization rates. Geochem. Cosmochim. Acta 347, 1–15. https://doi.org/10.1016/j.gca.2023.02.008.
- Lévy, D., Roche, V., Pasquet, G., Combaudon, V., Geymond, U., Loiseau, K., Moretti, I., 2023. Natural H₂ exploration: tools and workflows to characterize a play. Science and Technology for Energy Transition 78, 27. https://doi.org/10.2516/stet/ 2023021
- Lo Po, D., Braga, R., Massonne, H.J., Molli, G., Montanini, A., Bargossi, G., 2018. High-pressure tectono-metamorphic evolution of mylonites from the Variscan basement of the Northern Apennines, Italy. J. Metam. Geol. 36, 23–39. https://doi.org/10.1111/jmg.12281.
- Lo Po, D., Braga, R., Massonne, H.J., 2016. Petrographic, mineral and pressure-temperature constraints on phyllites from the Variscan basement at Punta Bianca, Northern Apennines, Italy. Italian Journal of Geosciences 135, 489–502. https://doi.org/10.3301/IJG.2015.29.
- Loiseati, K., Aubourg, C., Petit, V., Bordes, S., Lefeuvre, N., Thomas, E., et al., 2024. Hydrogen generation and heterogeneity of the serpentinization process at all scales: Turon de Técouère lherzolite case study, Pyrenees (France). Geoenergy 2 (1). https://doi.org/10.1144/geoenergy2023-024 geoenergy2023-024. Lopez-Lazaro, C., Bachaud, P., Moretti, I., Ferrando, N., 2019. Predicting the phase
- Lopez-Lazaro, C., Bachaud, P., Moretti, I., Ferrando, N., 2019. Predicting the phase behavior of hydrogen in NaCl brines by molecular simulation for geological applications. Bull. Soc. Geol. Fr. 190 (1). https://doi.org/10.1051/bsgf/2019008.
- Maiga, O., Deville, E., Laval, J., Prinzhofer, A., Diallo, A.B., 2023. Characterization of the spontaneously recharging natural hydrogen reservoirs of Bourakebougou in Mali. Sci. Rep. 13 (1), 11876. https://doi.org/10.1038/s41598-023-38977-y.
- Marroni, M., Pandolfi, L., 1996. The deformation history of an accreted ophiolite sequence: the Internal Liguride units (Northern Apennines, Italy). Geodin. Acta 9 (1), 13–29. https://doi.org/10.1080/09853111.1996.11417260.
- Marroni, M., Molli, G., Montanini, A., Tribuzio, R., 1998. The association of continental crust rocks with ophiolites (Northern Apennines, Italy): implications for the continent-ocean transition. Tectonophysics 292 (1–2), 43–66. https://doi.org/ 10.1016/S0040-1951(98)00060-2.
- Marroni, M., Meneghini, F., Pandolfi, L., 2010. Anatomy of the Ligure-Piemontese subduction system: evidence from late cretaceous–middle Eocene convergent margin deposits in the Northern Apennines, Italy. Int. Geol. Rev. 52 (10–12), 1160–1192. https://doi.org/10.1080/00206810903545493.
- Marroni, M., Meneghini, F., Pandolfi, L., 2017. A revised subduction inception model to explain the Late Cretaceous, double-vergent orogen in the precollisional western Tethys: evidence from the Northern Apennines. Tectonics 36, 2227–2249. https://doi.org/10.1002/2017TC004627.
- Marroni, M., Meneghini, F., Pandolfi, L., Hobbs, N., Luvisi, E., 2019. The Ottone-Levanto line of Eastern liguria (Italy) uncovered: a late Eocene-early Oligocene snapshot of northern apennine geodynamics at the alps/apennines junction. Episodes 42 (2), 107–118. https://doi.org/10.18814/epiiugs/2019/019009.
- Martinelli, G., Cremonini, S., Samonati, E., 2012. Geological and geochemical setting of natural hydrocarbon emissions in Italy. In: Al-Megren, H. (Ed.), Advances in Natural Gas Technology. InTech, p. 556. https://doi.org/10.5772/37446.
- Martinelli, G., Dadomo, A., Italiano, F., Petrini, R., Slejko, F.F., 2017. Geochemical monitoring of the 2012 Po Valley seismic sequence: a review and update. Chem. Geol. 469, 147–162. https://doi.org/10.1016/j.chemgeo.2016.12.013.
- Mattioli, M., Di Battistini, G., Zanzucchi, G., 2002. Petrology, geochemistry and age of the volcanic clasts from the Canetolo Unit (Northern Apennines, Italy). Boll. Soc. Geol. Ital. 1, 399–416.
- Milkov, A.V., Etiope, G., 2018. Revised genetic diagrams for natural gases based on a global dataset of> 20,000 samples. Org. Geochem. 125, 109–120. https://doi.org/ 10.1016/j.orggeochem.2018.09.002.

- Molli, G., 2008. Northern Apennine–Corsica orogenic system: an updated overview. htt
- Molli, G., Montanini, A., Frank, W., 2002. MORB-derived Variscan amphibolites in the Northern Apennine basement: the Cerreto metamorphic slices (Tuscan-Emilian Apennine, NW Italy). Ofioliti 27, 17–30. https://doi.org/10.4454/ofioliti.v27i1.171.
- Molli, G., Crispini, L., Malusà, M.G., Mosca, P., Piana, F., Federico, L., 2010. Geology of the Western Alps-Northern Apennine junction area: a regional review. In: Beltrando, Marco, Peccerillo, A., Mattei, M., Conticelli, S., Doglioni, C. (Eds.), J. Virtual Explor. https://doi.org/10.3809/jvirtex.2010.00215, 36 paper 10.
- Molli, G., Brogi, A., Caggianelli, Enrico, C., Liotta, D., Spina, A., Zibra, I., 2020. Late Palaeozoic tectonics in Central Mediterranean: a reappraisal. Swiss J. Geosci. 113, 23. https://doi.org/10.1186/s00015-020-00375-1.
- Montanini, A., Tribuzio, R., Anczkiewicz, R., 2006. Exhumation history of a garnet pyroxenite-bearing mantle section from a continent-ocean transition (Northern Apennine ophiolites, Italy). J. Petrol. 47 (10), 1943–1971. https://doi.org/10.1093/petrology/egl032.
- Montanini, A., Tribuzio, R., Vernia, L., 2008. Petrogenesis of basalts and gabbros from an ancient continent-ocean transition (External Liguride ophiolites, Northern Italy). Lithos 101, 453–479. https://doi.org/10.1016/j.lithos.2007.09.007.
- Moretti, I., Brouilly, E., Loiseau, K., Prinzhofer, A., Deville, E., 2021a. Hydrogen emanations in intracratonic areas: new guide lines for early exploration basin screening. Geosciences 11 (3), 145. https://doi.org/10.3390/geosciences11030145.
- Moretti, I., Prinzhofer, A., Françolin, J., Pacheco, C., Rosanne, M., Rupin, F., Mertens, J., 2021b. Long-term monitoring of natural hydrogen superficial emissions in a brazilian cratonic environment. Sporadic large pulses versus daily periodic emissions. Int. J. Hydrogen Energy 46 (5), 3615–3628. https://doi.org/10.1016/j. ijhydene.2020.11.026.
- Myagkiy, A., Moretti, I., Brunet, F., 2020. Space and time distribution of subsurface H₂ concentration in so-called "fairy circles". Insight from a conceptual 2-D transport model, BSGF 191, 13. https://doi.org/10.1051/bsgf/2020010.
- Neubeck, A., Duc, N.T., Bastviken, D., Crill, P., Holm, N.G., 2011. Formation of H₂ and CH₄ by weathering of olivine at temperatures between 30 and 70 C. Geochem. Trans. 12, 1–10. https://doi.org/10.1186/1467-4866-12-6.
- Ogata, K., Pini, G.A., Carè, D., Zélic, M., Dellisanti, F., 2012. Progressive development of block-in-matrix fabric in a shale-dominated shear zone: insights from the Bobbio Tectonic Window (Northern Apennines, Italy). Tectonics 31 (1). https://doi.org/10.1029/2011TC002924.
- Ojeda, L., Etiope, G., Jiménez-Gavilán, P., Martonos, I.M., Röckmann, T., Popa, M.E., Sivan, M., Castro-Gamez, A.F., Benavente, J., Vadillo, I., 2023. Combining methane clumped and bulk isotopes, temporal variations in molecular and isotopic composition, and hydrochemical and geological proxies to understand methane's origin in the Ronda peridotite massifs (Spain). Chem. Geol. 642, 121799. https:// doi.org/10.1016/j.chemgeo.2023.121799.
- Osselin, F., Soulaine, C., Fauguerolles, C., Gaucher, E.C., Scaillet, B., Pichavant, M., 2022. Orange hydrogen is the new green. Nature Geoscience15 (10), 765–769. https://doi.org/10.1038/s41561-022-01043-9.
- Pandeli, E., Gianelli, G., Puxeddu, M., Elter, F.M., 1994. The Palaeozoic basement of the Northern Apennines: stratigraphy, tectono-metamorphic evolution and Alpine hydrothermal process. Mem. Soc. Geol. It. 48, 627–654.
- Pasquet, G., Loiseau, K., Diatta, M., Firpo, G., Swire, P., Amey, A., Burckhart, T., Moretti, I., 2025. Natural hydrogen in the northern semail ophiolite: a case study in the emirate of Ras Al Khaimah. UAE. IJHE. https://doi.org/10.1016/j. iihydene 2025 02 259
- Piazza, A., Artoni, A., Ogata, K., 2016. The epiligurian wedge-top succession in the Enza Valley (Northern Apennines): evidence of a syn-depositional transpressive system. Swiss J. Geosci. 109, 17–36. https://doi.org/10.1007/s00015-016-0211-x.
- Piazza, A., Tinterri, R., Artoni, A., 2020. The role of orogen-transversal tectonic structures on "syn" and "post" depositional evolution of a foredeep succession: the case of the Cervarola Sandstones Formation, Miocene, Northern Apennines, Italy. Tectonophysics 778, 228367. https://doi.org/10.1016/j.tecto.2020.228367.
- Prinzhofer, A., Cissé, C.S.T., Diallo, A.B., 2018. Discovery of a large accumulation of natural hydrogen in Bourakebougou (Mali). Int. J. Hydrogen Energy 43 (42), 19315–19326. https://doi.org/10.1016/j.ijhydene.2018.08.193.
- Rampone, E., Hofmann, A.W., Piccardo, G.B., Vannucci, R., Bottazzi, P., Ottolini, L., 1995. Petrology, mineral and isotope geochemistry of the External Liguride peridotites (Northern Apennines, Italy). J. Petrol. 36, 81–105. https://doi.org/ 10.1093/petrology/36.1.81.
- Röckmann, T., Eyer, S., van der Veen, C., Popa, M.E., Tuzson, B., Monteil, G., Houweling, S., Harris, E., Brunner, D., Fischer, H., Zazzeri, G., Lowry, D., Nisbet, E. G., Brand, W.A., Necki, J.M., Emmenegger, L., Mohn, J., 2016. In situ observations of the isotopic composition of methane at the Cabauw tall tower site. Atmos. Chem. Phys. 16 (16), 10469–10487. https://doi.org/10.5194/acp-16-10469-2016.
- Salvioli-Mariani, E., Boschetti, T., Toscani, L., Montanini, A., Petriglieri, J.R., Bersani, D., 2020. Multi-stage rodingitization of ophiolitic bodies from Northern Apennines (Italy): constraints from petrography, geochemistry and thermodynamic modelling. Geosci. Front. 11 (6), 2103–2125. https://doi.org/10.1016/j.gsf.2020.04.017.
- Sanfilippo, A., Tribuzio, R., 2011. Melt transport and deformation history in a nonvolcanic ophiolitic section, northern Apennines, Italy: implications for crustal

- accretion at slow spreading settings. Geochem. Geophys. Geosyst. 12, Q0AG04. https://doi.org/10.1029/2010GC003429.
- Sanfilippo, A., Borghini, G., Rampone, E., Tribuzio, R., 2014. The Ligurian ophiolites: a journey through the building and evolution of slow spreading oceanic lithosphere. GFT (Geological Field Trips, Serv. Geol. It., ISPRA 6, 46. https://doi.org/10.3301/GFT.2014.06
- Schettino, A., Turco, E., 2011. Tectonic history of the western Tethys since the Late Triassic. Geol. Soc. Am. Bull. 123, 89–105. https://doi.org/10.1130/B30064.1.
- Schwarzenbach, E., 2011. Serpentinization, fluids and life: comparing carbon and sulfur cycles in modern and ancient environments. Doctoral dissertation, ETH Zurich). https://doi.org/10.3929/ethz-a-6560203.
- Sciarra, A., Cinti, D., Pizzino, L., Procesi, M., Voltattorni, N., Mecozzi, S., Quattrocchi, F., 2013. Geochemistry of shallow aquifers and soil gas surveys in a feasibility study at the Rivara natural gas storage site (Po Plain, Northern Italy). Appl. Geochem. 34, 3–22. https://doi.org/10.1016/j.apgeochem.2012.11.008.
- Scicli, A., 1972. L'Attività Estrattiva E Le Risorse Minerarie Della regione-Emilia-Romagna (Extractive Activity and Mineral Resources of the Emilia-Romagna Region). Pacini Editore, Modena, p. 728.
- Segadelli, S., Vescovi, P., Ogata, K., Chelli, A., Zanini, A., Boschetti, T., Petrella, E., Toscani, L., Gargini, A., Celico, F., 2017a. A conceptual hydrogeological model of ophiolitic aquifers (serpentinised peridotite): the test example of mt. Prinzera (Northern Italy). Hydrol. Process. 31 (5), 1058–1073. https://doi.org/10.1002/ hyp.11090.
- Segadelli, S., Vescovi, P., Chelli, A., Petrella, E., De Nardo, M.T., Gargini, A., Celico, F., 2017b. Hydrogeological mapping of heterogeneous and multi-layered ophiolitic aquifers (Mountain Prinzera, northern Apennines, Italy). J. Maps 13 (2), 737–746. https://doi.org/10.1080/17445647.2017.1376228.
- Servizio Geologico d'Italia, 1997. Carta geologica D'Italia Alla Scala 1:50.000, F. 197 Bobbio. ISPRA. https://doi.org/10.15161/oar.it/149922.
- Stampfli, G.M., Borel, G.D., 2002. A plate tectonic model for the Paleozoic and Mesozoic constrained by dynamic plate boundaries and restored synthetic oceanic isochrons. Earth Planet Sci. Lett. 196, 17–33. https://doi.org/10.1016/S0012-821X(01)00588-y
- Suda, K., Ueno, Y., Yoshizaki, M., Nakamura, H., Kurokawa, K., Nishiyama, E., et al., 2014. Origin of methane in serpentinite-hosted hydrothermal systems: the CH₄–H₂–H₂O hydrogen isotope systematics of the Hakuba Happo hot spring. Earth Planet Sci. Lett. 386, 112–125. https://doi.org/10.1016/j.epsl.2013.11.001.
- Szponar, N., Brazelton, W.J., Schrenk, M.O., Bower, D.M., Steele, A., Morrill, P.L., 2013. Geochemistry of a continental site of serpentinization, the Tablelands Ophiolite, Gros Morne National Park: a Mars analogue. Icarus 224 (2), 286–296. https://doi. org/10.1016/j.jcarus.2012.07.004.
- Tassi, F., Fiebig, J., Vaselli, O., Nocentini, M., 2012. Origins of methane discharging from volcanic-hydrothermal, geothermal and cold emissions in Italy. Chem. Geol. 310, 36–48. https://doi.org/10.1016/j.chemgeo.2012.03.018.
- Templeton, A.S., Ellison, E.T., Kelemen, P.B., Leong, J., Boyd, E.S., Colman, D.R., Matter, J.M., 2024. Low-temperature hydrogen production and consumption in partially-hydrated peridotites in Oman: implications for stimulated geological hydrogen production. Front. Geochem. 2, 1366268. https://doi.org/10.3389/ fronz.3024.1366688
- Tribuzio, R., Molli, G., Riccardi, M.P., Messiga, B., 1997. Poliphase metamorphism in ophiolitic gabbros from Bonassola (Internal Liguride Units, northern Apennines): a record of western Tethys oceanization. Ofioliti 22, 163–174.
- Tribuzio, R., Garzetti, F., Corfu, F., Tiepolo, M., Renna, M.R., 2016. U-Pb zircon geochronology of the Ligurian ophiolites (Northern Apennine, Italy): implications for continental breakup to slow seafloor spreading. Tectonophysics 666, 220–243. https://doi.org/10.1016/j.tecto.2015.10.024.
- Umezawa, T., Brenninkmeijer, C.A.M., Röckmann, T., van der Veen, C., Tyler, S.C., Fujita, R., Morimoto, S., Aoki, S., Sowers, T., Schmitt, J., Bock, M., Beck, J., Fischer, H., Michel, S.E., Vaughn, B.H., Miller, J.B., White, J.W.C., Brailsford, G., Schaefer, H., Sperlich, P., Brand, W.A., Rothe, M., Blunier, T., Lowry, D., Fisher, R.E., Nisbet, E.G., Rice, A.L., Bergamaschi, P., Veidt, C., Levin, I., 2018. Interlaboratory comparison of δ^{13C} and δD measurements of atmospheric CH₄ for combined use of data sets from different laboratories. Atmos. Meas. Tech. 11 (2), 1207–1231. https://doi.org/10.5194/amt-11-1207-2018.
- Van Hisenberg, D.J.J., Torsvik, T.H., Schmid, S.M., Matenco, L.C., Maffione, M., Vissers, R.L.M., Gurer, D., Spakman, W., 2020. Orogenic architecture of the Mediterranean region and kinematic reconstruction of its tectonic evolution since the Triassic. Gondwana Res. 81, 79–299. https://doi.org/10.1016/j.gr.2019.07.009.
- Vitale Brovarone, A., Martinez, I., Elmaleh, A., Compagnoni, R., Chaduteau, C., Ferraris, C., Esteve, I., 2017. Massive production of abiotic methane during subduction evidenced in metamorphosed ophicarbonates from the Italian Alps. Nat. Commun. 8 (1), 14134. https://doi.org/10.1038/ncomms14134.
- Zgonnik, V., 2020. The occurrence and geoscience of natural hydrogen: a comprehensive review. Earth Sci. Rev. 203, 103140. https://doi.org/10.1016/j. earscirev.2020.103140.
- Zgonnik, V., Beaumont, V., Deville, E., Larin, N., Pillot, D., Farrell, K.M., 2015. Evidence for natural molecular hydrogen seepage associated with Carolina bays (surficial, ovoid depressions on the Atlantic Coastal Plain, Province of the USA). Prog. Earth Planet. Sci. 2, 1–15. https://doi.org/10.1186/s40645-015-0062-5.